

Detected climate change signals in atmospheric circulation: mechanisms, puzzles and opportunities

Tiffany A Shaw¹, Julie M. Arblaster², Thomas Birner³, Amy Hawes Butler⁴, Daniela I.V. Domeisen⁵, Chaim I Garfinkel⁶, Hella Garny⁷, Kevin M Grise⁸, and Alexey Yurievich Karpechko⁹

¹University of Chicago

²Monash University

³Ludwig-Maximilians University

⁴NOAA Chemical Sciences Laboratory

⁵ETH Zurich

⁶Hebrew University of Jerusalem

⁷Deutsches Zentrum für Luft- und Raumfahrt

⁸University of Virginia

⁹Finnish Meteorological Institute

October 09, 2024

1
2
3
4
5
6
7
8
9
10
11
12
13
14
15
16
17
18
19
20
21
22
23
24
25
26

Emerging climate change signals in atmospheric circulation

T. A. Shaw¹, J. M. Arblaster², T. Birner^{3,8}, A. H. Butler⁴, D. I.V. Domeisen^{5,6}, C.I. Garfinkel⁷, H. Garny⁸, K. M. Grise⁹, and A. Yu. Karpechko¹⁰

¹The University of Chicago, Chicago, IL, USA.

²ARC Centre of Excellence for the Weather of the 21st Century, Monash University, Victoria, Australia.

³Ludwig-Maximilians-University Munich, Munich, Germany.

⁴National Oceanic and Atmospheric Administration, Chemical Sciences Laboratory, Boulder, CO, USA.

⁵Université de Lausanne, Lausanne, Switzerland

⁶ETH Zurich, Zurich, Switzerland

⁷Fredy & Nadine Herrmann Institute of Earth Sciences, The Hebrew University of Jerusalem, Israel.

⁸Deutsches Zentrum für Luft- und Raumfahrt, Oberpfaffenhofen, Germany,

⁹University of Virginia, Charlottesville, VA, USA

¹⁰Finnish Meteorological Institute, Helsinki, Finland.

Corresponding author: Tiffany Shaw (tas1@uchicago.edu)

Key Points:

- Long term trends in atmospheric circulation are emerging across different regions and seasons with some attributed to human activities.
- Many circulation signals have been linked to dynamical mechanisms involving thermodynamic changes, although discrepancies remain.
- Emerging signals in combination with new tools promise considerable progress in understanding the dynamical response in the coming decade.

27 Abstract

28 The circulation response to climate change shapes regional climate and extremes. Over the last
29 decade an increasing number of atmospheric circulation signals have been documented, with
30 some attributed to human activities. The circulation signals represent an exciting opportunity for
31 improving our understanding of dynamical mechanisms, testing our theories and reducing
32 uncertainties. The signals have also presented puzzles that represent an opportunity for better
33 understanding the circulation response to climate change, its contribution to climate extremes,
34 interactions with moisture, and connection to thermodynamic discrepancies. The next decade is
35 likely to be a golden age for dynamics with many advances possible.

36 Plain Language Summary

37 Regional climate change signals in atmospheric circulation (wind and pressure) have been
38 documented in many regions. Some of the signals are expected and have been attributed to
39 human activities whereas others are not. The next decade represents an exciting time to better
40 understand the dynamical mechanisms underlying these signals and their relationship to
41 thermodynamic signals with the goal of improving regional climate prediction.

42 1 Introduction

43 The emergence and attribution of thermodynamic signals in response to anthropogenic climate
44 change is well appreciated. Indeed global-mean warming over land and ocean, amplified
45 warming in the tropical upper troposphere, rising of the tropopause, cooling of the stratosphere,
46 regional land warming, and Arctic amplification of surface warming have all been attributed to
47 human activities (IPCC 2021). Thermodynamically driven changes in regional hot extremes,
48 heavy precipitation and drought have also been confidently attributed to human activities in
49 some regions (IPCC 2021, Fig. SPM.3). This progress on thermodynamic signals has been
50 achieved through a multi-pronged approach: detection of observed signals, attribution to human
51 activities, and understanding of the underlying mechanisms using climate model simulations that
52 exhibit fidelity in the signal and mechanisms.

53 Atmospheric circulation is well-known to affect regional climate through changes in
54 fluid-dynamic variables, including atmospheric wind, pressure. These changes can subsequently
55 influence moisture, clouds and radiation. Many generations of climate models have predicted
56 robust circulation responses to climate change by the end of the century, including an upward
57 shift and acceleration of the subtropical jet streams, weakening and expansion of the Hadley
58 circulation, poleward shifts of the eddy-driven jet streams, strengthening of the storm tracks in

59 the Southern Hemisphere and seasonally varying storm track responses in the Northern
60 Hemisphere. In general, circulation signals are more uncertain as compared to thermodynamic
61 ones, especially at the regional scale, due to large internal variability and the lack of sufficiently
62 strong constraints on atmospheric dynamics (Shepherd, 2014). Furthermore, competing
63 influences on dynamics in a changing climate, e.g. Arctic versus tropical warming, cloud
64 shortwave versus longwave responses, aerosol cooling versus greenhouse gas warming, etc also
65 can lead to a weak net dynamical response (Perlwitz 2012, Shaw et al., 2016). Hence dynamic
66 variables are considered to have a lower signal-to-noise ratio, which has cascading impacts on
67 hydrological cycle signals (Elbaum et al 2022).

68 Over the last decade an increasing number of atmospheric circulation signals, here
69 defined as statistically significant linear trends over the satellite era or longer, have been
70 documented in the literature. These signals are part of a growing number of regional climate
71 change signals, some of which exhibit discrepancies with model predictions (Shaw et al. 2024).
72 Here we focus specifically on atmospheric circulation signals that have been documented in the
73 literature since recent assessments (IPCC 2021, Shepherd 2014). We specifically highlight
74 signals that have emerged and been attributed to human activities; discuss progress on
75 understanding dynamical mechanisms underlying the signals; and describe remaining puzzles,
76 including the role of internal variability versus the forced response versus observational
77 uncertainty, model-observation discrepancies and the impact of mean state biases. We discuss
78 the importance of linking statistical analysis and understanding of dynamic and thermodynamic
79 signals. In particular, some thermodynamic signals exhibit discrepancies with model predictions,
80 e.g. the “pattern effect” of SST trends, and are potentially linked to the atmospheric circulation,
81 e.g. via thermodynamic gradients and cloud radiative effects. Finally, we highlight how
82 circulation signals, along with existing and emerging tools, represent an exciting opportunity for
83 making progress in the next few decades on understanding the dynamical mechanisms behind the
84 circulation response to climate change.

85 **2 Circulation signals**

86 The number of atmospheric circulation signals reported in the literature across different regions,
87 hemispheres, and seasons has grown significantly in recent years (Table 1). Some are zonal-
88 mean signals (8 out of 20) but many are regional (12 out of 20). For example, increased sea-

89 level pressure near South-West Western Australia is associated with recent drying trends in this
90 region (Fig. 1a,c,e; Hope et al 2006). Furthermore, many Southern Hemisphere signals are
91 zonally symmetric, leading to similar impacts across longitudinal regions (Kang et al. 2024).

92 In some cases the signals have been detected and attributed to human activities (see
93 below and Table 1). In other cases the role of internal variability and/or reanalysis biases still
94 needs to be assessed. In many cases the sign of the signal is consistent with model predictions,
95 however in some cases there is a discrepancy between observations and models. In still other
96 cases, expected regional signals, like reduced precipitation in the Central and Western
97 Mediterranean associated with higher sea-level pressure, will take more time to emerge (Fig.
98 1b,d,f) (Seager et al. 2024).

99 One of the earliest examples of an atmospheric circulation signal being formally
100 attributed to human activities involved ozone depletion (Gillett et al., 2013). The circulation
101 signals include an increase in the strength of the winds in the southern hemisphere stratosphere,
102 an associated delay of the spring-time breakdown of the stratospheric polar vortex, and a
103 poleward shift of the eddy-driven tropospheric jet stream (Fig. 2) and southern Hadley cell edge
104 in austral summer (Thompson et al. 2011, Lee & Feldstein 2013, WMO 2018). Since the 2000s,
105 ozone recovery, which opposes the influence of greenhouse gas increases on the circulation, has
106 been associated with reduced SH circulation trends (Banerjee et al 2020, Zambri et al. 2021),
107 though these are sensitive to end points (Fig. 2).

108 In recent years several more atmospheric circulation signals have been attributed to
109 human activities (Table 1), including greenhouse gas emissions, but also with ozone depletion or
110 aerosol emissions either in isolation or in combination (e.g. Gillett et al., 2016). In the Northern
111 Hemisphere the combination of anthropogenic greenhouse gas and aerosol emissions have
112 weakened the summertime circulation as measured by the zonal-mean storm tracks (eddy kinetic
113 energy, Chemke & Coumou 2024), zonal-mean jet stream, and regional surface cyclone activity
114 (mean sea level pressure, Kang et al. 2024b). Improved estimates of anthropogenic aerosol
115 forcing were important for the improved Northern Hemisphere summertime storm track signals
116 in CMIP5 versus CMIP6 (Chemke & Coumou 2024). The weakening of the East Asian

117 summertime jet stream has been attributed exclusively to anthropogenic aerosol emissions (Dong
118 et al. 2022).

119 The weakening of the annual-mean Northern Hemisphere Hadley cell has also been
120 attributed to anthropogenic greenhouse gas and aerosol emissions (Chemke & Yuval 2023,
121 Lionello et al. 2024). The poleward shift of the Southern Hemisphere Hadley cell edge has been
122 attributed to ozone depletion and anthropogenic greenhouse gas emissions (Grise et al. 2019;
123 Lionello et al. 2024).

124 **3 Progress in understanding mechanisms**

125 Many dynamical mechanisms have been proposed to explain atmospheric circulation responses
126 to anthropogenic forcing that have been robustly predicted by generations of climate models
127 (Thompson et al. 2011, Vallis et al. 2015, Hoskins & Woollings 2015, Shaw, 2019, Wills et al.
128 2019). Here we highlight progress on understanding mechanisms underlying the response to
129 ozone depletion, greenhouse gas and aerosol forcing as they relate to the circulation signals listed
130 in Table 1.

131

132 **3.1 Ozone depletion**

133 Ozone depletion reduces the shortwave absorption of ultraviolet radiation, cooling the lower
134 stratosphere. This cooling induces an increase of the meridional temperature gradient and a
135 strengthening of the stratospheric zonal wind consistent with thermal wind balance. Imposing a
136 cooling of the lower stratosphere in idealized model simulations leads to a poleward shift of the
137 tropospheric eddy-driven jet (Polvani & Kushner 2002, Kushner & Polvani 2004, Butler et al.
138 2010). However, the tropospheric response to stratospheric forcing is sensitive to the state of the
139 troposphere (Chan & Plumb, 2009; Garfinkel et al. 2013). A mechanism proposed to explain the
140 poleward shift of the eddy-driven jet stream in the lower atmosphere links the change in
141 stratospheric winds to a modification of the eastward propagation of tropospheric eddies thereby
142 affecting the momentum flux (Chen & Held 2007). At this time, there is still not a complete
143 mechanistic understanding that connects the ozone hole to the shift of the jet stream and Hadley
144 cell edge (Thompson et al. 2011, Kidston et al. 2015). This lack of understanding may in part be

145 due to the complex dynamical interactions that are found to be crucial for a downward impact
146 (Kidston et al. 2015).

147

148 **3.2 Greenhouse gas forcing**

149 Greenhouse gas increases lead to tropical upper tropospheric warming consistent with moist
150 adiabatic adjustment (Manabe & Wetherald, 1975, Held 1993). This response increases the
151 meridional temperature gradient near the tropopause, strengthening the subtropical jet and shear
152 via thermal wind balance (Allen & Sherwood, 2008; Lee et al., 2019). This direct impact of the
153 tropics on the atmospheric circulation is confirmed by a CO₂ increase only in the tropics in
154 model simulations (Shaw & Tan 2018, Shaw, 2019).

155 The shift of the jet stream and Hadley cell in response to greenhouse gas increases have
156 been argued to be connected to this tropical warming response (Lorenz & DeWeaver, 2007; Lu
157 et al. 2007; Lu et al., 2014; Butler et al., 2010). However the poleward shift of the midlatitude
158 near-surface jet and Hadley cell edge and the strengthening of the subtropical jet happen on
159 distinct timescales (compare red and blue lines in Fig. 3), suggesting the shifts are driven by
160 different mechanisms (Chemke & Polvani, 2019, 2021; Menzel et al., 2019). Recent studies
161 suggest midlatitude processes including local moisture gradient, latent heat release, vertical
162 temperature gradient (static stability), and cloud changes are more important than tropical
163 changes (Shaw & Voigt, 2016, Voigt & Shaw, 2016, Chemke & Polvani 2019, 2021, Garfinkel
164 et al., 2024; Lachmy, 2022; Tamarin-Brodsky & Kaspi, 2017; Tan & Shaw, 2020; Voigt et al.,
165 2021). The importance of moisture and clouds has been revealed by advancing theory to
166 incorporate moisture (e.g., Tamarin-Brodsky & Kaspi, 2017; Shaw et al. 2018, Lachmy, 2022)
167 and simulations across the model hierarchy (Garfinkel et al 2024; Ghosh et al., 2024, Tan &
168 Shaw 2020, Ceppi & Hartmann, 2016; Voigt & Shaw, 2015).

169 The signal of Northern Hemisphere summertime circulation weakening has been linked
170 to a weakening of the near-surface temperature gradient due to Arctic amplification (Coumou et
171 al. 2015), however recent work shows the contribution of Arctic sea ice loss and Arctic
172 amplification to the circulation signal is negligible (Blackport et al, 2019; Blackport & Screen,
173 2021; Kang et al. 2023). Instead the weakening signal is related to high latitude warming over
174 land (not ocean or sea ice) induced by greenhouse gas and aerosol forcing (Dong et al., 2022;
175 Chemke & Coumou 2024, Kang et al., 2024b).

176 The strengthening of the Southern Hemisphere wintertime storm tracks, which occurs
177 robustly across all longitudes, has been connected to several mechanisms: An increase in mean
178 available potential energy due to increased latitudinal temperature gradients aloft (O’Gorman
179 2010); increased surface flux trends that reflect equatorward ocean energy transport and
180 Southern Ocean cooling (Shaw et al. 2022); and changes in the vertical structure of the jet stream
181 (Chemke et al. 2022).

182 Mechanisms explaining regional signals are related to stationary wave changes. The
183 strengthening summertime Northern Hemisphere stationary wave signal has been connected to a
184 teleconnection from the tropical Pacific (Sun et al. 2022) and soil moisture deficits (Teng et al.
185 2022). A related signal is the increase in extratropical heatwaves in summertime (e.g., Russo &
186 Domeisen, 2023, Domeisen et al. 2023), which have been suggested to be related to increased
187 “waviness” of the jet stream and the increased occurrence of so-called resonance events
188 (Kornhuber et al., 2017; Mann et al., 2018), often associated with double jets (Rousi et al., 2022).
189 However the quantitative mechanism underlying this link has not been established. Instead,
190 anthropogenic aerosol forcing has been argued to be important for regional heat wave signals
191 (Schumacher et al. 2024).

192 During wintertime the strengthening high over the Mediterranean has been connected to
193 the large-scale upper-tropospheric circulation and land-sea contrast response, and specifically to
194 a less rapid warming of the Mediterranean sea than of the surrounding land (Tuel & Eltahir
195 2020). The large-scale tropospheric circulation response consists of an eastward shift of
196 wintertime stationary waves associated with strengthened eastward subtropical upper-level jet
197 (Simpson et al., 2016; Wills et al 2019). This eastward shift is associated with uncertainty in
198 regional climate change in e.g., Western North America (Simpson et al., 2016). Finally, the
199 pattern of sea surface temperature warming can modify regional circulation and subtropical
200 precipitation responses to greenhouse gas forcing (Zappa et al 2020).

201

202 **3.3 Aerosol forcing**

203 The mechanism proposed to explain the regional circulation signals in response to aerosol
204 forcing involves the aerosol direct effect (aerosol-radiation interactions). Regions with
205 reductions in aerosol optical depth, e.g. Eurasia and Eastern North America, show increases in
206 clear-sky surface shortwave radiation (unmasking effect) whereas regions with increases in

207 aerosol optical depth, e.g. South and East Asia, show a decrease in clear-sky surface shortwave
208 radiation. The surface radiation signals weaken the meridional surface temperature gradient
209 from the tropics to the extratropics, which following thermal wind balance weakens the
210 summertime Eurasian jet. The shortwave radiation signals are coupled via the longitudinal
211 circulation to the downstream ocean leading to a weakening of the storm tracks (Kang et al.
212 2024b).

213 Other studies have proposed additional mechanisms linked to the indirect influence of
214 aerosols on clouds. For example, sulfate aerosols may brighten clouds which reflect more
215 radiation to space, leading to a change in radiative balance that promotes poleward heat transport
216 by the atmosphere and ocean (Needham & Randall, 2023).

217

218 **4 Puzzles**

219 **4.1 Model-observation discrepancies**

220 The lengthening observational record has provided some “puzzles” where there are apparent
221 discrepancies between observed and modeled signals (Shaw et al. 2024). There are several well-
222 known thermodynamic discrepancies, including opposite signed SST trends in observations and
223 models in the tropical Pacific (Lee et al., 2022; Seager et al. 2022; Wills et al., 2022) and
224 Southern Ocean (Wills et al., 2022; Kang et al., 2023).

225 In addition, important circulation discrepancies have been identified. In particular, the
226 Walker circulation trend is toward a strengthening in observations but a weakening in models
227 (Chung et al., 2019). Also, there is a strengthening of the Northern Hemisphere Hadley cell in
228 reanalysis data but a weakening in models, though there is evidence that the reanalysis trends are
229 artificial (Chemke & Polvani 2019b).

230 Similar to thermodynamic discrepancies, there are also cases where models capture the
231 signal but it is underestimated as compared to reanalysis trends even after accounting for internal
232 variability: increased Southern Hemisphere storminess trends (Chemke et al., 2022; Shaw et al.,
233 2022) and North Atlantic lower-tropospheric jet strength trend (Blackport & Fyfe 2022, compare
234 model distributions in colors to black line representing reanalysis in Fig. 4). In other cases the
235 models overestimate the trends (strengthening of the upper-tropospheric jet stream; Woollings et
236 al., 2023).

237 The relationship between thermodynamic and dynamic discrepancies is an active area of
238 research. Recent papers show SST trend discrepancies impact Southern Hemisphere storminess
239 and midlatitude jet trends (Yang et al., 2021; Kang et al., 2024), and heatwave trends over
240 Europe are underestimated in models due to a discrepancy in the dynamical contribution
241 (compare black dots representing models to colored lines representing observations in Fig. 5),
242 although the details of this circulation trend discrepancy are not well understood and remain to
243 be investigated (Vautard et al., 2023).

244 An important limitation of atmospheric circulation signals that needs to be taken into
245 account when comparing model and observed signals is that atmospheric circulation signals rely
246 heavily on reanalysis products. Such datasets can exhibit drifts and jumps due to changes in the
247 underlying data sources (SPARC, 2022). In the Southern Hemisphere there is considerable
248 spread in circulation signals across these products (Martineau et al. 2024, Kang et al. 2024). In
249 the Northern Hemisphere, diabatic heating biases in reanalysis products have been shown to
250 impact Hadley cell signals (Chemke & Polvani 2019). Surface pressure observations have been
251 used to resolve the discrepancy in Hadley cell signals (Chemke & Yuval 2023).

252

253 **4.2 Disentangling forced response from internal variability**

254 One of the major challenges in comparing observed and model circulation signals is the
255 confounding factors of internal variability, which can mask or exacerbate forced trends in the
256 climate system, and observational uncertainty. For example, recent work for the Brewer-Dobson
257 circulation trends shows that observational uncertainty can be large enough to account for the
258 discrepancy with simulated Brewer-Dobson circulation trends in the middle stratosphere (Garny
259 et al, submitted to RoG).

260 One way to separate the forced response from internal variability is using single forcing
261 simulations. For example, if the signal is present in response to greenhouse gas or aerosol forcing
262 only, and observational and model uncertainty is low, then it is likely a forced response. If the
263 signal is present in the experiments without anthropogenic forcing (e.g. the preindustrial control
264 experiment), then one cannot rule out the role of internal variability. Another way to quantify the
265 role of internal variability is using large ensemble simulations with identical external forcing and
266 slightly different initial conditions (Deser et al., 2020; Maher et al., 2021). The two approaches
267 are combined in single-forcing large ensembles, which have been used to reconcile some

268 discrepancies (by accounting for internal variability), such as the poleward expansion of the
269 Hadley cell edge documented in the late 2000s (Grise et al., 2019) or cold winters over subpolar
270 Eurasia from 1998 to 2012 (Garfinkel et al 2017; Outten et al 2022). However, given the
271 relatively large magnitude of internal variability at regional scales (particularly in the
272 extratropics during wintertime) and potential model errors, acknowledging a range of plausible
273 future circulation trends (“storylines”) is necessary for impacts planning (Zappa & Shepherd,
274 2017; Mindlin et al., 2020; Schmidt & Grise, 2021; Williams et al., 2024).

275 While large ensembles can help disentangle the signal from the noise, recent work has
276 highlighted a signal-to-noise issue in coupled models suggesting that models may not properly
277 represent the magnitude of forced signals relative to internal variability. This “signal-to-noise
278 paradox” manifests most clearly when the ensemble-mean signal correlates better with
279 observations of the real world than with individual members of the initialized model forecast
280 ensemble (Weisheimer et al. 2024).

281

282 **4.3 Role of mean state biases/spread for future change**

283 The spread in model climatologies has been used to constrain thermodynamic climate change
284 signals, e.g. the snow-ice albedo feedback (Hall and Qu 2006), through emergent constraints.
285 Emergent constraints are statistical relationships between a model’s representation of a particular
286 physical process in the current climate and its future projection. Emergent constraints are most
287 robust when they are supported by a plausible physical mechanism.

288 Several emergent constraints have been proposed for circulation signals (Simpson et al.,
289 2021): for example, the Southern Hemisphere eddy-driven jet position (Kidston & Gerber,
290 2010), and the wintertime stationary wave response over the North Pacific (Simpson et al.,
291 2016). In both cases, a mechanism was proposed to explain the emergent constraint: fluctuation
292 dissipation theorem for jet position, and jet stream strength affecting stationary wavelength.
293 Unfortunately, some dynamical emergent constraints are not robust across CMIP versions (Wu et
294 al., 2019; Curtis et al., 2020; Karpechko et al. 2024). Furthermore, the Southern Hemisphere jet
295 position constraint, which is only robust in wintertime (Simpson & Polvani, 2016), appears to be
296 an artifact of the zonal mean (Breul et al., 2023).

297 Mean state model biases can have important implications for the forced response. For
298 example, even if a model accurately simulates the observed circulation response to climate

299 change (e.g., a poleward shift of the eddy-driven jet stream), if the circulation feature does not
300 have the correct location or magnitude in the present-day climate, then the model's projected
301 future climate change signal may be biased in terms of location and/or magnitude (Maraun et al.,
302 2017; Grise, 2022). Systematically addressing this issue globally is challenging and requires a
303 detailed understanding of the circulation features for all relevant regions.

304 **5 Opportunities for progress**

305 Understanding the emerging circulation signals and unraveling the puzzles they present provide
306 exciting opportunities for making progress in understanding the dynamical response to climate
307 change. Some opportunities for future research are:

308

309 **5.1 Investigate signals across the seasonal cycle**

310 Almost all of the dynamical signals in Table 1 are for the winter and summer seasons.
311 Investigating signals in other seasons such as autumn and spring as well as seasonal transitions is
312 important. During these seasons some signals may be stronger (Watt-Meyer et al., 2019) because
313 there potentially exist fewer competing thermodynamic signals.

314 It is also unclear how climate change affects the seasonal cycle of dynamical features
315 beyond the monsoons, which exhibit a well-documented delay in response to climate change
316 (e.g., Seth et al., 2013) and the stratospheric polar vortex, which is projected to form earlier and
317 decay later in the future (Ayarzaguena et al., 2020; Rao and Garfinkel 2021). Quantifying and
318 understanding the seasonality of dynamical changes has important implications for impacts such
319 as severe weather, ecosystems, forest fires, and agriculture.

320

321 **5.2 Move beyond the longitudinal and time mean**

322 Almost all of the dynamical signals in Table 1 reflect the time-mean. Circulation extremes have
323 received only limited attention beyond blocking. Yet, recent work suggests the signal of climate
324 change may be larger in the tails of the circulation distribution (Shaw & Miyawaki, 2024). It is
325 also important to understand how circulation trends affect trends in other variables such as heat
326 waves (Vautard et al., 2023).

327 Along similar lines, for a wide range of extremes and processes, there is much work to be
328 done to understand how the dynamical response to climate change varies across different

329 regions. For example, insights have been gained into recent trends by defining the Hadley Cell
330 for different regional sectors (Nguyen et al., 2018; Staten et al., 2019; Hoskins et al., 2020;
331 Gillett et al., 2021). The well-known model-observation discrepancy in tropical SST trends
332 (Wills et al. 2022, Seager et al. 2022) represents an opportunity for understanding how tropical
333 climate change affects regional circulation trends and this should be investigated further.
334 Ultimately, teleconnections bridging different regions will change due to mean state changes
335 under climate change and more work is needed to understand how.

336

337 **5.3 Use signals to test mechanisms and model fidelity**

338 Now that circulation signals are emerging, the dynamical mechanisms underlying the circulation
339 trends can be compared to theoretical expectations and model predictions. Applying the
340 numerous theoretical frameworks that have been proposed to explain dynamical responses to
341 climate change (Vallis et al. 2015, Hoskins & Woollings 2015, Shaw, 2019, Wills et al. 2019)
342 offers great potential for progress. Large ensemble, single forcing simulations (Smith et al. 2022)
343 can also be leveraged to attribute observed circulation changes, to investigate whether internal
344 variability involves dynamical mechanisms that are distinct from the forced response to
345 anthropogenic climate change, to clarify the relative importance of different anthropogenic
346 forcings, to showcase examples where models lack fidelity, to isolate and potentially correct
347 signal-to-noise biases (section 4.2), and to directly examine how climate forcings affect the tails
348 of the distribution (e.g. section 5.2).

349

350 **5.4 Leverage the power of existing and emerging tools**

351 Existing tools such as idealized models (Schemm & Röthlisberger, 2024; Jiménez-Esteve &
352 Domeisen, 2022; Jiménez-Esteve et al, 2022), model hierarchies (Maher et al, 2019), mechanism
353 denial experiments targeted toward understanding circulation signals and nudging (Hitchcock et
354 al. 2022) are all powerful for understanding mechanisms and unraveling the relationship between
355 circulation signals and other trends, or to understand the role of mean-state biases in the
356 atmospheric circulation (e.g. Friesen et al., 2022). The impacts of known thermodynamic biases,
357 e.g. SST trend biases, can be understood and quantified through targeted model experiments, e.g.
358 using pacemaker simulations with coupled models (Kang et al. 2024).

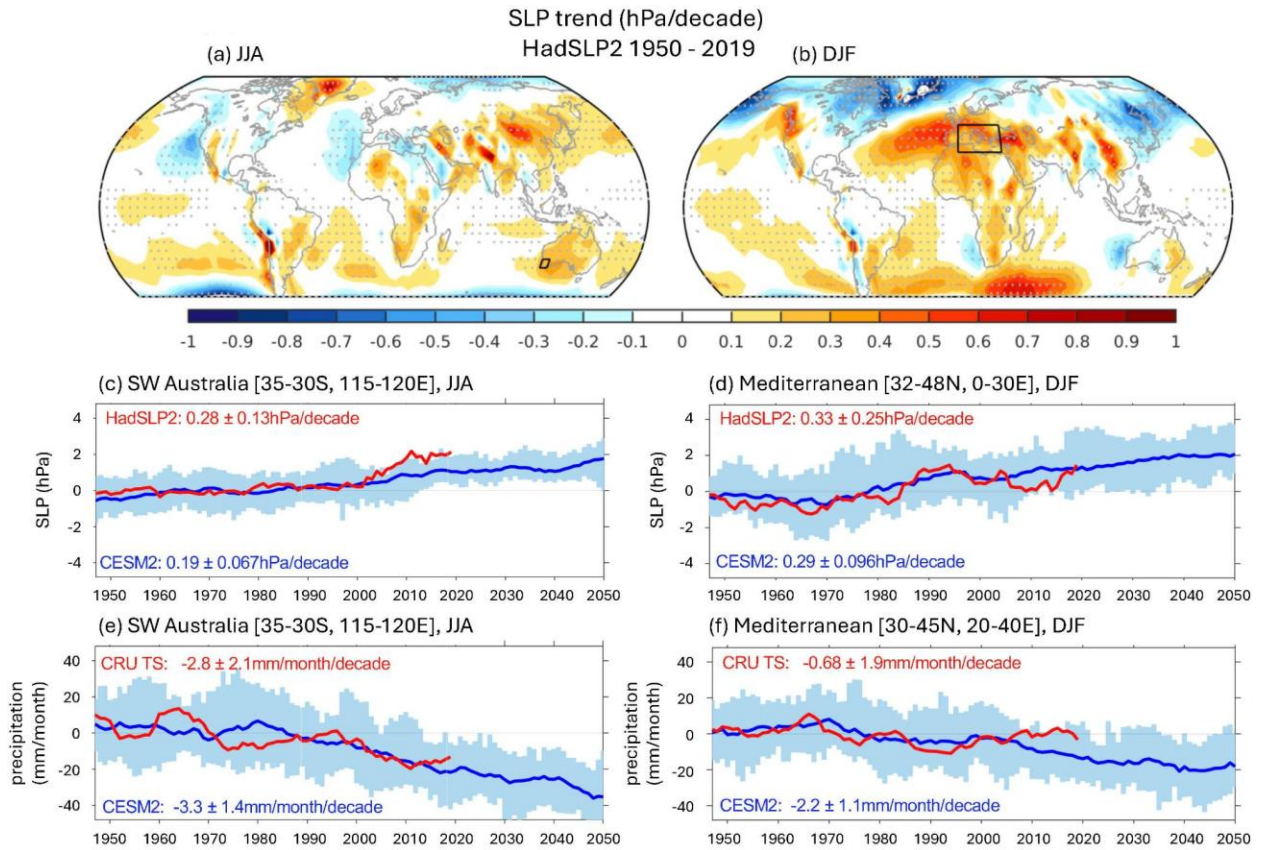
359 Several new tools have emerged in the last decade that can be leveraged for making
360 progress. Subseasonal to seasonal (S2S) forecasting models has emerged as a more widespread
361 tool, with large ensembles of S2S forecasts that can be leveraged for understanding dynamical
362 mechanisms and model-observation discrepancies. By pooling different ensemble members and
363 different initializations for a given target forecast, and by assuming that atmospheric initial
364 conditions are lost within the first month, tens of thousands of potential realizations of climate
365 can be created (e.g. Kelder et al., 2020; Kolstad et al., 2022). This method could be exploited to
366 improve mechanistic understanding of data-limited dynamical processes such as teleconnections.
367 S2S ensemble forecasts can additionally be used to diagnose common model biases that also
368 exist on climate timescales (L’Heureux et al., 2022; Garfinkel et al 2022; Lawrence et al, 2022;
369 Beverley et al., 2023; Randall & Emanuel, 2024).

370 The use of AI/ML methods has exploded in the last few years. Physics-informed and
371 explainable AI has the potential to advance our understanding of circulation signals (Connolly et
372 al. 2023). In particular, these methods may be able to “learn” the source of discrepancies
373 between models and observations, and structural uncertainties across different models.

374 Finally, high resolution global models going down to kilometer scale resolution present
375 an exciting opportunity for understanding how large- and small-scale dynamics interact. In order
376 to answer outstanding questions, carefully designed mechanistic model experiments across the
377 model hierarchy are still crucial, which should be informed by results from new high-resolution
378 (or large ensemble) model experiments. High resolution models also have the potential to reveal
379 where model-observation discrepancies are the result of not properly representing small-scale
380 dynamics in both the atmosphere and ocean.

381 A new era of climate change research is upon us, one where atmospheric circulation
382 signals are emerging, attribution is becoming possible and puzzles and discrepancies are
383 accumulating. There is an opportunity to embrace these signals and the puzzles they present,
384 including cases where there is a lack of consensus, and use the signals as an opportunity to
385 further advance our understanding of the climate system and improve predictions of regional
386 climate change.

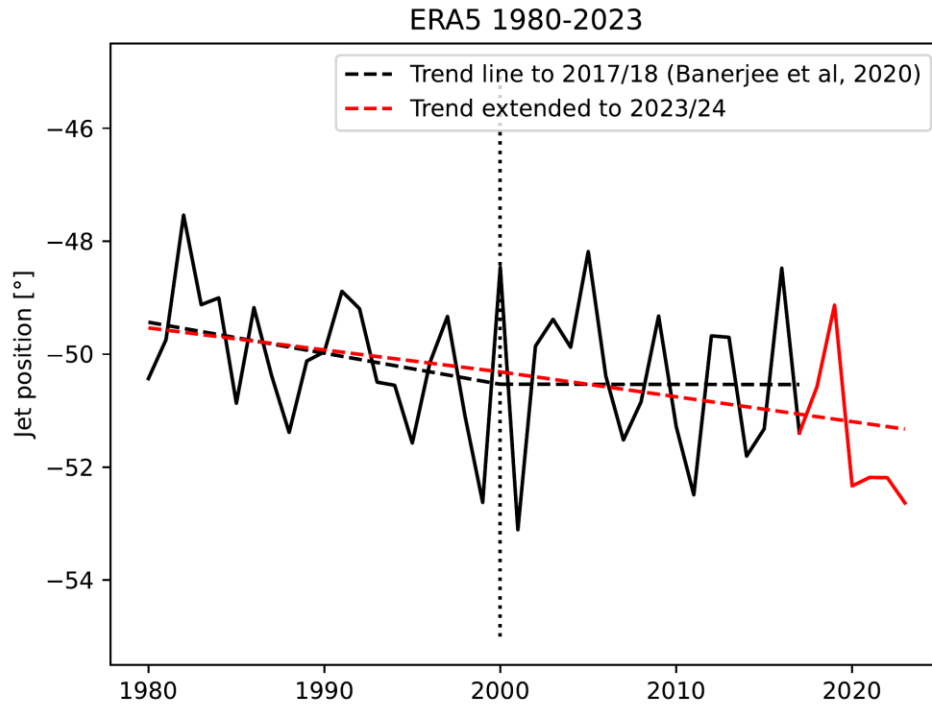
387



388

389 Figure 1: Regional circulation signals for JJA (left) and DJF (right). (a,b) Spatial structure of
 390 SLP trends [hPa/decade] from 1950-2019 in observations with stippling indicating statistically
 391 significant linear trends at the 0.05 level. Time series of (c) SLP [hPa] and (e) precipitation
 392 [mm/month] anomalies in observations (red line, HadSLPv2 for SLP, and CRU TS v4.07 for
 393 precipitation) over South-West Australia (black box in a) during JJA. (d,f) DJF SLP and
 394 precipitation over Mediterranean regions (black box in b) defined in Tuel and Eltahir (2020).
 395 Mean (blue line) and range (blue shading) of the 15-member historical-GHG only simulation in
 396 CESM2 of SLP and precipitation (Simpson et al 2023). All time series have been smoothed with
 397 a 10-year running mean.

398



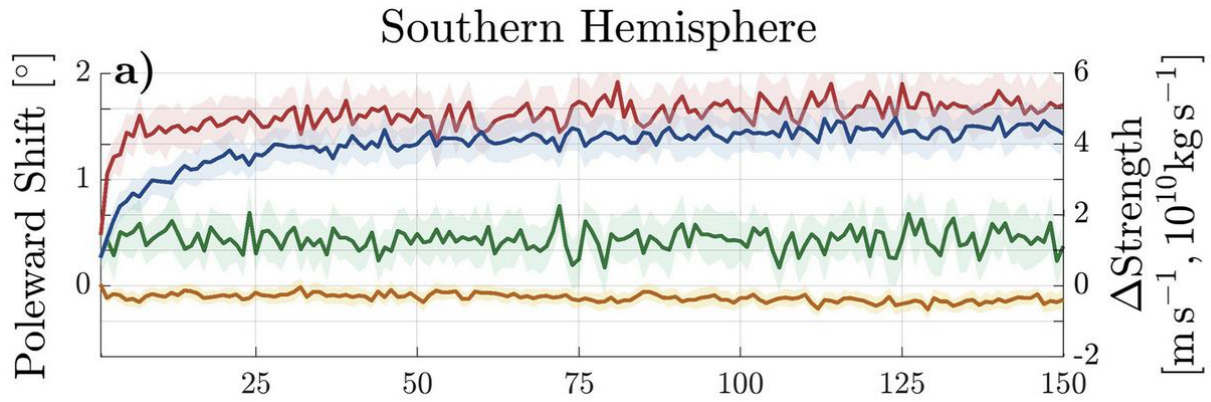
399

400 Figure 2: SH mid-latitude jet stream position response to ozone depletion. Jet position in DJF
401 from ERA5, reproducing Banerjee et al. 2020, for years 1980/81-2017/18 (black lines), and
402 extended time series to 2023/24 (red lines). Trends are fitted by continuous piecewise linear
403 regression (following Banerjee et al), and trend values are $-0.5^{\circ}/\text{dec}$ for the ozone depletion
404 period (1980/81 to 2000/01), and $0.0^{\circ}/\text{dec}$ for 2000/01-2017/18. For the extended time series,
405 trend values are $-0.4^{\circ}/\text{dec}$ for both ozone depletion and recovery periods, emphasizing the
406 sensitivity of trend estimates from short records to end points.

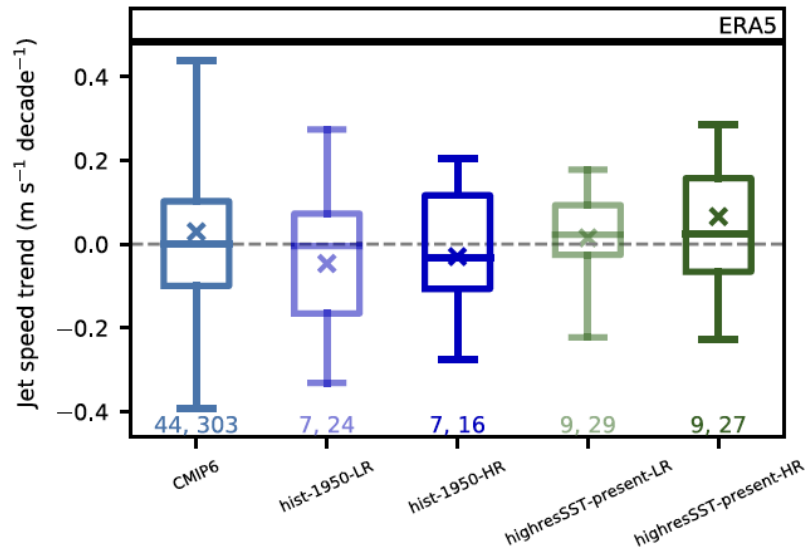
407

408

409

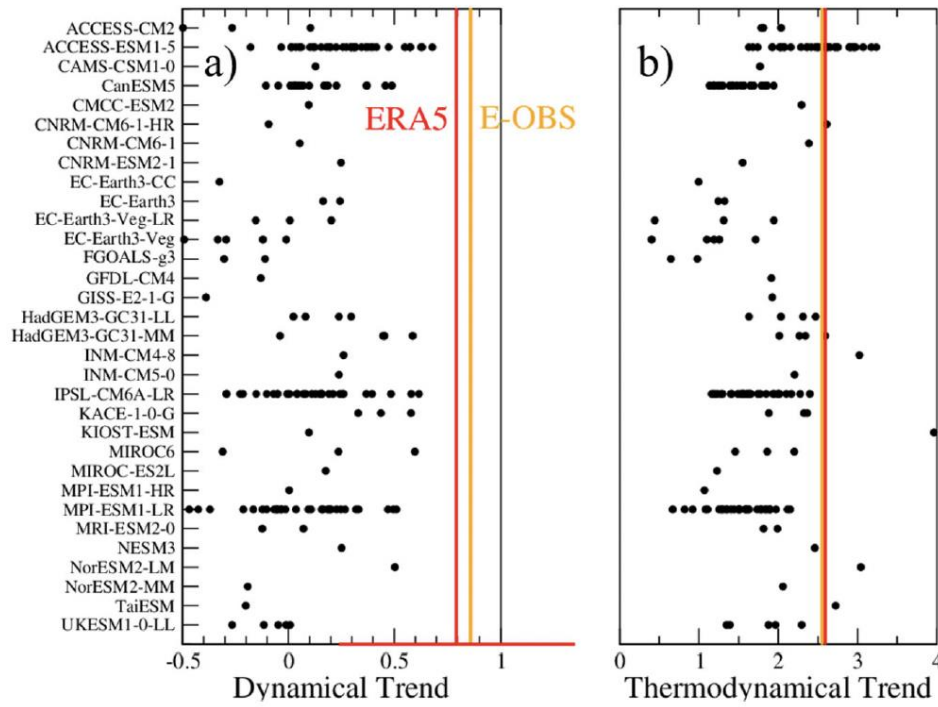


410
 411 Figure 3: Time series of southern hemispheric response in model years to quadrupling
 412 atmospheric CO₂ for (a) the Hadley cell (HC) edge (red) and strength (orange) and the
 413 subtropical jet (STJ) location (green) and strength (blue). For each plot, shading represents the
 414 95% confidence interval of model spread. Taken from Menzel et al. (2019).
 415



416
 417 Figure 4: Trends in North Atlantic lower-tropospheric (700 hPa) jet stream strength from 1951-
 418 2014 in reanalysis data (ERA5) and across coupled (CMIP6) climate model ensemble, and low
 419 (LR) and high (HR) resolution HighResMIP climate model ensemble. The box represents upper
 420 and lower quartile ranges, and the whiskers represent the minimum and maximum
 421 from all ensemble members. The lines in the boxes indicate the median from all
 422 ensembles, and the crosses represent the multimodel mean. The two numbers at the bottom

423 indicate the total number of models (left) and total number of ensemble members (right) from
 424 each experiment. Taken from Blackport & Fyfe (2022).



425
 426 Figure 5: Dynamical (a) and thermodynamical (b) contributions to the summer TX_x (summer
 427 maximum of maximal daily temperature) trends from ERA5 ECMWF Reanalysis (red line), E-
 428 OBS observation (orange line), and the 170 CMIP6 model simulations
 429 (names in ordinate) that were available (black dots) averaged over Western Europe.
 430 The thermodynamical contributions are simply calculated as residual by subtracting
 431 the dynamical trend from the total trend. For reference, the red bar
 432 at the bottom of (a) represents the 95% confidence interval of the estimate of the ERA5 TX_x
 433 dynamical trend, estimated with a Gaussian assumption, i. e. the interval
 434 is calculated as plus or minus 2* the standard deviation (STD) of the error estimate
 435 on the trend coefficient. This confidence range describes the uncertainty related to
 436 the internal variability. This shows that this confidence range, calculated with the
 437 single realization of the observation, is consistent with the uncertainty range calculated
 438 from simulation members (respective standard deviations for observed
 439 trend and simulated trends of 0.28 and 0.25). Taken from Vautaurd et al. (2023).

440 **Acknowledgments**

441 The authors acknowledge the participants of the WCRP APARC DynVar/SNAP Workshop that
442 took place 9-13 October 2023 in Munich, Germany. TAS acknowledges support from NSF
443 (AGS-2300037) and NOAA (NA23OAR4310597). Support from the Swiss National Science
444 Foundation through project PP00P2_198896 to DD is gratefully acknowledged. This project has
445 received funding from the European Research Council (ERC) under the European Union's
446 Horizon 2020 research and innovation programme (Grant agreement No. 847456). CIG
447 acknowledges the support of the Israel Science Foundation (grant agreement 1727/21). KMG
448 acknowledges support from NSF (AGS-2330009). JMA acknowledges support from the ARC
449 Centre of Excellence for the Weather of the 21st Century (CE230100012) and partial support
450 from the Regional and Global Model Analysis component of the Earth and Environmental
451 System Modelling Program of the U.S. Department of Energy's Office of Biological and
452 Environmental Research via National Science Foundation IA 1947282. AYK acknowledges
453 support from the European Union's Horizon 2020 research and innovation framework
454 programme under Grant agreement 774101003590 (PolarRES).

455 **Open Research**

456 No data was generated.

457 **Conflict of Interest**

458 The authors declare no conflicts of interest relevant to this study.

459 **References**

460 Allen, R. J., & Sherwood, S. C. (2008). Warming maximum in the tropical upper troposphere deduced from thermal
461 winds. *Nature Geoscience*, 1, 399.

- 462 Allen, R. J., Sherwood, S. C., Norris, J. R., & Zender, C. S. (2012). Recent Northern Hemisphere tropical expansion
463 primarily driven by black carbon and tropospheric ozone. *Nature*, 485(7398), 350–354.
464 <https://doi.org/10.1038/nature11097>
- 465 Ayarzagüena, B., Charlton-Perez, A. J., Butler, A. H., Hitchcock, P., Simpson, I. R., Polvani, L. M., et al. (2020).
466 Uncertainty in the response of sudden stratospheric warmings and stratosphere-troposphere coupling to
467 quadrupled CO₂ concentrations in CMIP6 models. *Journal of Geophysical Research: Atmospheres*, 125,
468 e2019JD032345. <https://doi.org/10.1029/2019JD032345>
- 469 Banerjee, A., Fyfe, J. C., Polvani, L. M., Waugh, D., & Chang, K.-L. (2020). A pause in Southern Hemisphere
470 circulation trends due to the Montreal Protocol. *Nature*, 579(7800), 544–548.
471 <https://doi.org/10.1038/s41586-020-2120-4>
- 472 Beverley, J. D., Newman, M., & Hoell, A. (2023). Rapid development of systematic ENSO-related seasonal forecast
473 errors. *Geophysical Research Letters*, 50, e2022GL102249. <https://doi.org/10.1029/2022GL102249>
- 474 Blackport, R., Screen, J. A., van der Wiel, K., & Bintanja, R. (2019). Minimal influence of reduced Arctic sea ice on
475 coincident cold winters in mid-latitudes. *Nature climate change*, 9(9), 697-704.
- 476 Blackport, R., & Screen, J. A. (2021). Observed statistical connections overestimate the causal effects of Arctic sea
477 ice changes on midlatitude winter climate. *Journal of Climate*, 34(8), 3021-3038.
- 478 Blackport, R., & Fyfe, J.C. (2022). Climate models fail to capture strengthening wintertime North Atlantic jet and
479 impacts on Europe. *Science Advances*, 8, eabn3112. <https://doi.org/10.1126/sciadv.abn3112>
- 480 Borowiak, A., A. King, T. Lane, The link between the Madden-Julian Oscillation and rainfall trends in
481 northwest Australia, *Geophysical Research Letters*, 50 (2023), 10.1029/2022GL101799e2022GL101799
- 482 Breul, P., Ceppi, P., & Shepherd, T. G. (2023). Revisiting the wintertime emergent constraint of the southern
483 hemispheric midlatitude jet response to global warming. *Weather and Climate Dynamics*, 4, 39–47.
484 <https://doi.org/10.5194/wcd-4-39-2023>, 2023.
- 485 Butler, A. H., Thompson, D. W. J., & Heikes, R. (2010). The Steady-State Atmospheric Circulation Response to
486 Climate Change–like Thermal Forcings in a Simple General Circulation Model. *Journal of Climate*, 23(13),
487 3474–3496. <https://doi.org/10.1175/2010JCLI3228.1>
- 488 Ceppi, P., & Hartmann, D. L. (2016). Clouds and the Atmospheric Circulation Response to Warming. *Journal of*
489 *Climate*, 29(2), 783–799. <https://doi.org/10.1175/JCLI-D-15-0394.1>

- 490 Chan, C. J., & Plumb, R. A. (2009). The response to stratospheric forcing and its dependence on the state of the
491 troposphere. *Journal of the Atmospheric Sciences*, 66(7), 2107-2115.
- 492 Chang, E. K. M., Ma, C.-G., Zheng, C. & Yau, A.M.W. (2016). Observed and projected decrease in Northern
493 Hemisphere extratropical cyclone activity in summer and its impacts on maximum temperature.
494 *Geophysical Research Letters*, 43, 2200–2208. <https://doi.org/10.1002/2016GL068172>
- 495 Chemke, R., & Polvani, L. M. (2019b). Opposite tropical circulation trends in climate models and in reanalyses.
496 *Nature Geoscience*, 12(7), 528–532. <https://doi.org/10.1038/s41561-019-0383-x>
- 497 Chemke, R., & Polvani, L. M. (2019). Exploiting the Abrupt 4 x CO₂ Scenario to Elucidate Tropical
498 Expansion Mechanisms. *J. Climate*, 32, 859–875.
- 499 Chemke, R., & Polvani, L. M. (2021). Elucidating the Mechanisms Responsible for Hadley Cell
500 Weakening Under 4 × CO₂ Forcing. *Geophys. Res. Lett.*, 10.1029/2020GL090348
- 501 Chemke, R., & Yuval, J. (2023). Human-induced weakening of the Northern Hemisphere tropical circulation.
502 *Nature* 617, 529–532. <https://doi.org/10.1038/s41586-023-05903-1>
- 503 Chemke, R., & Coumou, D. (2024). Human influence on the recent weakening of storm tracks in boreal
504 summer. *npj Climate and Atmos. Sci.* 10.1038/s41612-024-00640-2
- 505 Chemke, R., Polvani, L. M., Kay, J. E., & Orbe, C. (2021). Quantifying the role of ocean coupling in Arctic
506 amplification and sea-ice loss over the 21st century. *Npj Climate and Atmospheric Science*, 4(1), 1–9.
507 <https://doi.org/10.1038/s41612-021-00204-8>
- 508 Chemke, R., Ming, Y. & Yuval, J. (2022). The intensification of winter mid-latitude storm tracks in the Southern
509 Hemisphere. *Nature Climate Change*, 12, 553–557. <https://doi.org/10.1038/s41558-022-01368-8>
- 510 Chung, E.-S., Timmermann, A., Soden, B. J., Ha, K.-J., Shi, L., & John, V. O. (2019). Reconciling opposing
511 Walker circulation trends in observations and model projections. *Nature Climate Change*, 9(5), 405–412.
512 <https://doi.org/10.1038/s41558-019-0446-4>
- 513 Connolly, C., E. A. Barnes, P. Hassanzadeh, M. Pritchard (2023) Using neural networks to learn the jet
514 stream forced response from natural variability, *Artificial Intelligence for the Earth Systems* 2 (2), e220094
- 515 Coumou, D., Di Capua, G., Vavrus, S., Wang, L., & Wang, S. (2018). The influence of Arctic amplification on mid-
516 latitude summer circulation. *Nature Communications*, 9(1), 2959. [https://doi.org/10.1038/s41467-018-](https://doi.org/10.1038/s41467-018-05256-8)
517 05256-8

- 518 Coumou, D., Lehmann, J., & Beckmann, J. (2015). The weakening summer circulation in the Northern Hemisphere
519 mid-latitudes. *Science*, 348(6232), 324–327. <https://doi.org/10.1126/science.1261768>
- 520 Cox, T., Donohoe, A., Armour, K. C., Frierson, D. M. W. and G. H. Roe. (2024). Trends in Atmospheric Heat
521 Transport Since 1980. *J. Climate*, doi: 10.1175/JCLI-D-23-0385.1.
- 522 Curtis, P. E., Ceppi, P., & Zappa, G. (2020). Role of the mean state for the Southern Hemispheric jet stream
523 response to CO2 forcing in CMIP6 models. *Environmental Research Letters*, 15, 064011.
524 <https://doi.org/10.1088/1748-9326/ab8331>
- 525 Deser, C., Lehner, F., Rodgers, K.B., Ault, T., Delworth, T.L., DiNezio, P.N., et al. (2020). Insights from Earth
526 system model initial-condition large ensembles and future prospects. *Nature Climate Change*, 10, 277–286.
527 <https://doi.org/10.1038/s41558-020-0731-2>
- 528 Domeisen, D. I. V., Eltahir, E. A. B., Fischer, E. M., Knutti, R., Perkins-Kirkpatrick, S. E., Schär, C., Seneviratne, S.
529 I., Weisheimer, A., & Wernli, H. (2023). Prediction and projection of heatwaves. *Nature Reviews Earth &*
530 *Environment*, 4(1), 36–50. <https://doi.org/10.1038/s43017-022-00371-z>
- 531 Dong, B., Sutton, R. T., Shaffrey, L., & Harvey, B. (2022). Recent decadal weakening of the summer Eurasian
532 westerly jet attributable to anthropogenic aerosol emissions. *Nature Communications*, 13(1), 1148.
533 <https://doi.org/10.1038/s41467-022-28816-5>
- 534 Elbaum, E., Garfinkel, C. I., Adam, O., Morin, E., Rostkier-Edelstein, D., & Dayan, U. (2022). Uncertainty in
535 projected changes in precipitation minus evaporation: Dominant role of dynamic circulation changes and
536 weak role for thermodynamic changes. *Geophysical Research Letters*, 49, e2022GL097725.
537 <https://doi.org/10.1029/2022GL097725>
- 538 Eyring, V., et al., 2021: Human Influence on the Climate System. In *Climate Change 2021: The Physical*
539 *Science Basis. Contribution of Working Group I to the Sixth Assessment Report of the Intergovernmental*
540 *Panel on Climate Change* Cambridge University Press, Cambridge, United Kingdom and New York, NY,
541 USA, pp. 423–552, doi:10.1017/9781009157896.005.
- 542 Franzke, C. L. E., & Harnik, N. (2023). Long-Term Trends of the Atmospheric Circulation and Moist Static Energy
543 Budget in the JRA-55 Reanalysis. *Journal of Climate*, 36(9), 2959-2984. [https://doi.org/10.1175/JCLI-D-](https://doi.org/10.1175/JCLI-D-21-0724.1)
544 [21-0724.1](https://doi.org/10.1175/JCLI-D-21-0724.1)
- 545 Garfinkel, C. I., Son, S. W., Song, K., Aquila, V. and Oman, L. D. (2013) The Effect of Tropospheric Jet Latitude

- 546 on Coupling between the Stratospheric Polar Vortex and the Troposphere. *J. Climate*, 26, 2077–2095.
- 547 Garfinkel, C. I., Son, S. W., Song, K., Aquila, V. and Oman, L. D. (2017) Stratospheric variability contributed to
548 and sustained the recent hiatus in Eurasian winter warming. *Geophysical research letters* 44, no. 1: 374-
549 382.
- 550 Garfinkel, C. I., Schwartz, C., Domeisen, D. I. V., Son, S.-W., Butler, A. H., & White, I. P. (2018). Extratropical
551 atmospheric predictability from the quasi-biennial oscillation in subseasonal forecast models. *Journal of*
552 *Geophysical Research: Atmospheres*, 123, 7855–7866. <https://doi.org/10.1029/2018JD028724>
- 553 Garfinkel, C. I., Chen, W., Li, Y., Schwartz, C., Yadav, P., & Domeisen, D. (2022). The Winter North Pacific
554 Teleconnection in Response to ENSO and the MJO in Operational Subseasonal Forecasting Models Is Too
555 Weak. *Journal of Climate*, 35(24), 8013-8030. <https://doi.org/10.1175/JCLI-D-22-0179.1>
- 556 Garfinkel, C. I., Keller, B., Lachmy, O., White, I., Gerber, E. P., Jucker, M., & Adam, O. (2024). Impact of
557 parameterized convection on the storm track and near-surface jet response to global warming: Implications
558 for mechanisms of the future poleward shift. *Journal of Climate*, 37, 2541–2564.
559 <https://doi.org/10.1175/JCLI-D-23-0105.1>
- 560 Garny, H., F. Ploeger, M. Abalos, H. Bönisch, A. Castillos, T. von Clarmann, M. Diallo, A. En-gels, J. C. Laube,
561 M. Linz, J. Neu, A. Podglajen, E. Ray, L. Rivoire, L. N. Saunders, G. Stiller, F. Voet, K. A. Walker: Age
562 of stratospheric air: Progress on processes, observations and long-term trends, *submitted to Reviews of*
563 *Geophysics*.
- 564 Gertler, C.G., & O’Gorman, P.A. (2019). Changing available energy for extratropical cyclones and associated
565 convection in Northern Hemisphere summer. *Proceedings of the National Academy of Sciences*, 116,
566 4105-4110. <https://doi.org/10.1073/pnas.1812312116>
- 567 Ghosh, S., Lachmy, O., & Kaspi, Y. (2024). The role of diabatic heating in the midlatitude atmospheric circulation
568 response to climate change. *Journal of Climate*, 1(aop). <https://doi.org/10.1175/JCLI-D-23-0345.1>
- 569 Gillett, N. P., J. C. Fyfe, and D. E. Parker (2013), Attribution of observed sea level pressure trends to
570 greenhouse gas, aerosol, and ozone changes, *Geophys. Res. Lett.*, 40, 2302–2306, doi:10.1002/grl.50500.
- 571 Gillett, N. P., Shiogama, H., Funke, B., Hegerl, G., Knutti, R., Matthes, K., Santer, B. D., Stone, D., & Tebaldi, C.
572 (2016). The Detection and Attribution Model Intercomparison Project (DAMIP v1.0) contribution to
573 CMIP6. *Geoscientific Model Development*, 9(10), 3685–3697. <https://doi.org/10.5194/gmd-9-3685-2016>

- 574 Gillett, Z. E., H. H. Hendon, J. M. Arblaster, and E.-P. Lim. (2021). Tropical and extratropical influences on the
575 variability of the Southern Hemisphere wintertime subtropical jet. *Journal of Climate*, **34**, 4009–4022,
576 <https://doi.org/10.1175/JCLI-D-20-0460.1>.
- 577 Grise, K. M. (2022). Atmospheric circulation constraints on 21st century seasonal precipitation storylines for the
578 southwestern United States. *Geophysical Research Letters*, **49**, e2022GL099443.
579 <https://doi.org/10.1029/2022GL099443>
- 580 Grise, K. M., Davis, S.M., Simpson, I.R., Waugh, D.W., Fu, Q., Allen, R.J., et al. (2019). Recent tropical
581 expansion: Natural variability or forced response? *Journal of Climate*, **32**, 1551–1571.
582 <https://doi.org/10.1175/JCLI-D-18-0444.1>
- 583 Hall, A., & Qu, X. (2006). Using the current seasonal cycle to constrain snow albedo feedback in future climate
584 change. *Geophysical Research Letters*, **33**, L03502. <https://doi.org/10.1029/2005GL025127>.
- 585 Hanna, E., Fettweis, X., & Hall, R. J. (2018). Brief communication: Recent changes in summer Greenland blocking
586 captured by none of the CMIP5 models. *The Cryosphere*, **12**, 3287–3292. [https://doi.org/10.5194/tc-12-](https://doi.org/10.5194/tc-12-3287-2018)
587 [3287-2018](https://doi.org/10.5194/tc-12-3287-2018)
- 588 Heidemann, H., Cowan, T., Henley, B.J., Ribbe, J., Freund, M. & Power, S. (2023) Variability and long-term
589 change in Australian monsoon rainfall: a review. *WIREs Climate Change*, **14**, e823.
- 590 Hitchcock, P. and Coauthors, 2022: Stratospheric Nudging And Predictable Surface Impacts (SNAPSI): a protocol
591 for investigating the role of stratospheric polar vortex disturbances in subseasonal to seasonal forecasts,
592 *Geo. Mod. Dev*, **15**, 5073–5092
- 593 Held, I. M. (1993), Large-Scale dynamics and climate change, *Bull. Amer. Met. Soc.*, **74**,
594 [doi:10.1175/1520-0477](https://doi.org/10.1175/1520-0477).
- 595 Hope, P. K., Drosowsky, W., and Nicholls, N. (2006): Shifts in the synoptic systems influencing
596 southwest Western Australia, *Clim. Dynam.*, **26**, 751–764, [https://doi.org/10.1007/s00382-006-0115-](https://doi.org/10.1007/s00382-006-0115-y)
597 [y](https://doi.org/10.1007/s00382-006-0115-y).
- 598 Hoskins, B., Woollings, T. (2015) Persistent Extratropical Regimes and Climate Extremes. *Curr Clim*
599 *Change Rep* **1**, 115–124. <https://doi.org/10.1007/s40641-015-0020-8>
- 600 Hoskins, B.J., Yang, G.-Y., & Fonseca, R.M. (2020). The detailed dynamics of the June–August Hadley Cell.
601 *Quarterly Journal of the Royal Meteorological Society*, **146**, 557–575. <https://doi.org/10.1002/qj.3702>

- 602 Huang, C. S. Y., & Nakamura, N. (2016). Local Finite-Amplitude Wave Activity as a Diagnostic of Anomalous
603 Weather Events. *Journal of the Atmospheric Sciences*, 73(1), 211-229. [https://doi.org/10.1175/JAS-D-15-](https://doi.org/10.1175/JAS-D-15-0194.1)
604 0194.1
- 605 IPCC (2021). *Climate Change 2021: The Physical Science Basis. Contribution of Working Group I to the Sixth*
606 *Assessment Report of the Intergovernmental Panel on Climate Change* [Masson-Delmotte, V., P. Zhai, A.
607 Pirani, S.L. Connors, C. Péan, S. Berger, N. Caud, Y. Chen, L. Goldfarb, M.I. Gomis, M. Huang, K.
608 Leitzell, E. Lonnoy, J.B.R. Matthews, T.K. Maycock, T. Waterfield, O. Yelekçi, R. Yu, and B. Zhou
609 (eds.)]. Cambridge University Press, Cambridge, United Kingdom and New York, NY, USA, In press,
610 doi:[10.1017/9781009157896](https://doi.org/10.1017/9781009157896).
- 611 Kang, J. M., Shaw, T. A., & Sun, L. (2023). Arctic Sea Ice Loss Weakens Northern Hemisphere Summertime
612 Storminess but Not Until the Late 21st Century. *Geophysical Research Letters*, 50(9), e2022GL102301.
613 <https://doi.org/10.1029/2022GL102301>
- 614 Kang, J. M., Shaw, T. A., Kang, S., Simpson, I. R. & Yu, Y. (2024). Revisiting the reanalysis-model
615 discrepancy in Southern Hemisphere winter storm track trends. [10.22541/essoar.171224128.81410474/v1](https://doi.org/10.22541/essoar.171224128.81410474/v1)
- 616 Kang, J. M., Shaw, T. A. and Sun, L. (2024b). Anthropogenic aerosols have significantly weakened the
617 regional summertime circulation in the Northern Hemisphere during the satellite era.
618 [10.22541/essoar.171901442.29170078/v1](https://doi.org/10.22541/essoar.171901442.29170078/v1)
- 619 Kang, S.M., Yu, Y., Deser, C., Zhang, X., Kang, I.-S., Lee, S.-S., Rodgers, K.B., & Ceppi, P. (2023). Global
620 impacts of recent Southern Ocean cooling. *Proceedings of the National Academy of Sciences*, 120,
621 e2300881120. <https://doi.org/10.1073/pnas.230088112>
- 622 Karpechko, A. Yu., Wu, Z., Simpson, I. R., Kretschmer, M., Afargan-Gerstman, H., Butler, A. H., Domeisen, D.
623 I.V., Garny, H., Lawrence, Z, Manzini, E., & Sigmond, M.: Northern Hemisphere Stratosphere-
624 Troposphere Circulation Change in CMIP6 1 Models. Part 2: Mechanisms and Sources of the Spread
625 (2024), *Journal of Geophysical Research: Atmospheres*, doi: [10.1029/2024JD040823](https://doi.org/10.1029/2024JD040823)
- 626 Kelder, T., Müller, M., Slater, L.J., Marjoribanks, T.I., Wilby, R.L., Prudhomme, C., Bohlinger, P., Ferranti, L., &
627 Nipen, T. (2020). Using UNSEEN trends to detect decadal changes in 100-year precipitation extremes. *npj*
628 *Climate and Atmospheric Science*, 3, 47. <https://doi.org/10.1038/s41612-020-00149-4>
- 629 Kidston, J., & Gerber, E.P. (2010). Intermodel variability of the poleward shift of the austral jet stream in the

- 630 CMIP3 integrations linked to biases in 20th century climatology. *Geophysical Research Letters*, 37,
 631 L09708. <https://doi.org/10.1029/2010GL042873>.
- 632 Kidston, J., Scaife, A., Hardiman, S. *et al.* Stratospheric influence on tropospheric jet streams, storm tracks and
 633 surface weather. *Nature Geosci* 8, 433–440 (2015). <https://doi.org/10.1038/ngeo2424>
- 634 Kornhuber, K., Petoukhov, V., Karoly, D., Petri, S., Rahmstorf, S., & Coumou, D. (2017). Summertime Planetary
 635 Wave Resonance in the Northern and Southern Hemispheres. *Journal of Climate*, 30(16), 6133–6150.
 636 <https://doi.org/10.1175/JCLI-D-16-0703.1>
- 637 Kolstad, E. W., Lee, S. H., Butler, A. H., Domeisen, D. I. V., & Wulff, C. O. (2022). Diverse surface signatures of
 638 stratospheric polar vortex anomalies. *Journal of Geophysical Research: Atmospheres*, 127,
 639 e2022JD037422. <https://doi.org/10.1029/2022JD037422>
- 640 Knutson, T. R. & Ploshay, J. Sea level pressure trends: model-based assessment of detection, attribution,
 641 and consistency with CMIP5 historical simulations. *J. Clim.* 34, 327–346 (2021).
- 642 Lachmy, O. (2022). The relation between the latitudinal shifts of midlatitude diabatic heating, eddy heat flux and the
 643 eddy-driven jet in CMIP6 models. *Journal of Geophysical Research: Atmospheres*, 127, e2022JD036556.
 644 <https://doi.org/10.1029/2022JD036556>
- 645 Lawrence, Z. D., Abalos, M., Ayarzagüena, B., Barriopedro, D., Butler, A. H., Calvo, N., ... & Wu, R. W. Y. (2022).
 646 Quantifying stratospheric biases and identifying their potential sources in subseasonal forecast systems.
 647 *Weather and Climate Dynamics, Weather Clim. Dynam.*, 3, 977–1001
- 648 Lee, S., & Feldstein, S.B. (2013). Detecting Ozone- and Greenhouse Gas–Driven Wind Trends with Observational
 649 Data. *Science*, 339,563-567. <https://doi.org/10.1126/science.1225154>
- 650 Lee, S., L’Heureux, M., Wittenberg, A.T., Seager, R., O’Gorman, P.A., & Johnson, N.C. (2022). On the
 651 future zonal contrasts of equatorial Pacific climate: Perspectives from Observations, Simulations, and
 652 Theories. *npj Climate and Atmospheric Science*, 5, 82. <https://doi.org/10.1038/s41612-022-00301-2>
- 653 Lee, S. H., Williams, P. D., & Frame, T. H. A. (2019). Increased shear in the North Atlantic upper-level jet stream
 654 over the past four decades. *Nature*, 572(7771), 639–642. <https://doi.org/10.1038/s41586-019-1465-z>
- 655 L’Heureux, M.L., Tippett, M.K., & Wang, W. (2022). Prediction Challenges From Errors in Tropical
 656 Pacific Sea Surface Temperature Trends. *Frontiers in Climate*, 4, 837483.
 657 <https://doi.org/10.3389/fclim.2022.837483>

- 658 Lionello, P., D'Agostino, R., Ferreira, D., Nguyen, H., & Singh, M. S. (2024). The Hadley circulation in a changing
659 climate. *Ann NY Acad Sci.*, 1534, 69–93. <https://doi.org/10.1111/nyas.15114>
- 660 Lorenz, D. J., & DeWeaver, E. T. (2007). Tropopause height and zonal wind response to global warming in the
661 IPCC scenario integrations. *Journal of Geophysical Research: Atmospheres*, 112(D10).
662 <https://doi.org/10.1029/2006JD008087>
- 663 Lorenz, D. J., & Hartmann, D. L. (2001). Eddy–Zonal Flow Feedback in the Southern Hemisphere. *Journal of the*
664 *Atmospheric Sciences*, 58(21), 3312–3327. [https://doi.org/10.1175/1520-](https://doi.org/10.1175/1520-0469(2001)058<3312:EZFFIT>2.0.CO;2)
665 [0469\(2001\)058<3312:EZFFIT>2.0.CO;2](https://doi.org/10.1175/1520-0469(2001)058<3312:EZFFIT>2.0.CO;2)
- 666 Lu, J., Leung, L. R., Yang, Q., Chen, G., Collins, W. D., Li, F., Hou, Z. J., & Feng, X. (2014). The robust dynamical
667 contribution to precipitation extremes in idealized warming simulations across model resolutions.
668 *Geophysical Research Letters*, 41, 2971–2978. <https://doi.org/10.1002/2014GL059532>
- 669 Maher, P., Gerber, E. P., Medeiros, B., Merlis, T. M., Sherwood, S., Sheshadri, A., ... & Zurita-Gotor, P. (2019).
670 Model hierarchies for understanding atmospheric circulation. *Reviews of Geophysics*, 57(2), 250–280.
- 671 Maher, N., Milinski, S., & Ludwig, R. (2021). Large ensemble climate model simulations: introduction, overview,
672 and future prospects for utilising multiple types of large ensemble. *Earth System Dynamics*, 12, 401–418.
673 <https://doi.org/10.5194/esd-12-401-2021>
- 674 Manabe, S., & Wetherald, R. T. (1975). The Effects of Doubling the CO₂ Concentration on the climate of a General
675 Circulation Model. *Journal of the Atmospheric Sciences*, 32(1), 3–15. [https://doi.org/10.1175/1520-](https://doi.org/10.1175/1520-0469(1975)032<0003:TEODTC>2.0.CO;2)
676 [0469\(1975\)032<0003:TEODTC>2.0.CO;2](https://doi.org/10.1175/1520-0469(1975)032<0003:TEODTC>2.0.CO;2)
- 677 Mann, M. E., Rahmstorf, S., Kornhuber, K., Steinman, B. A., Miller, S. K., Petri, S., & Coumou, D. (2018).
678 Projected changes in persistent extreme summer weather events: The role of quasi-resonant amplification.
679 *Science Advances*, 4(10). <https://doi.org/10.1126/sciadv.aat3272>
- 680 Maraun, D., Shepherd, T. G., Widmann, M., Zappa, G., Walton, D., Gutierrez, J. M., et al. (2017). Towards process-
681 informed bias correction of climate change simulations. *Nature Climate Change*, 7(11), 764–773.
682 <https://doi.org/10.1038/nclimate3418>
- 683 Martineau, P., Behera, S. K., Nonaka, M., Nakamura, H. & Kosaka, Y. (2024), ‘Seasonally dependent
684 increases in subweekly temperature variability over Southern Hemisphere landmasses detected in multiple
685 reanalyses’, *Weather and Climate Dynamics* 5(1), 1–15.

- 686 Menzel, M. E., Waugh, D., & Grise, K. (2019). Disconnect Between Hadley Cell and Subtropical Jet Variability and
687 Response to Increased CO₂. *Geophysical Research Letters*, *46*(12), 7045–7053.
688 <https://doi.org/10.1029/2019GL083345>
- 689 Mindlin, J., Shepherd, T.G., Vera, C.S., Osman, M., Zappa, G., Lee, R.W., & Hodges, K.I. (2020). Storyline
690 description of Southern Hemisphere midlatitude circulation and precipitation response to greenhouse gas
691 forcing. *Climate Dynamics*, *54*, 4399–4421. <https://doi.org/10.1007/s00382-020-05234-1>
- 692 Needham, M. R., & Randall, D. A. (2023). Anomalous Northward Energy Transport due to Anthropogenic Aerosols
693 during the Twentieth Century. *Journal of Climate*, *36*(19), 6713–6728. [https://doi.org/10.1175/JCLI-D-22-](https://doi.org/10.1175/JCLI-D-22-0798.1)
694 [0798.1](https://doi.org/10.1175/JCLI-D-22-0798.1)
- 695 Nguyen, H., Hendon, H. H., Lim, E. P., Boschhat, G., Maloney, E., & Timbal, B. (2018). Variability of the extent of
696 the Hadley circulation in the southern hemisphere: a regional perspective. *Climate Dynamics*, *50*(1-2), 129-
697 142. <https://doi.org/10.1007/s00382-017-3592-2>
- 698 O’Gorman, P. A. (2010). Understanding the varied response of the extratropical storm tracks to climate change.
699 *Proceedings of the National Academy of Sciences*, *107*(45), 19176–19180.
700 <https://doi.org/10.1073/pnas.1011547107>
- 701 Outten, S., Li C., King, M. P., Suo, L., Siew, P. Y., Davy, R., Dunn-Sigouin, E. et al. (2022) Reconciling
702 conflicting evidence for the cause of the observed early 21st century Eurasian cooling. *Weather and*
703 *Climate Dynamics Discussions* 2022: 1-32.
- 704 Perlwitz, J. Tug of war on the jet stream. *Nature Clim. Change* *1*, 29–31 (2012).
- 705 Randall, D. A., & Emanuel, K. (2024). The Weather–Climate Schism. *Bulletin of the American Meteorological*
706 *Society*, *105*(1), E300-E305. <https://doi.org/10.1175/BAMS-D-23-0124.1>
- 707 Rao, J., & Garfinkel, C. I. (2021). Projected changes of stratospheric final warmings in the Northern and Southern
708 Hemispheres by CMIP5/6 models. *Climate Dynamics*. <https://doi.org/10.1007/s00382-021-05647-6>
- 709 Rousi, E., Kornhuber, K., Beobide-Arsuaga, G., Luo, F., & Coumou, D. (2022). Accelerated western European
710 heatwave trends linked to more-persistent double jets over Eurasia. *Nature Communications*, *13*(1), 3851.
711 <https://doi.org/10.1038/s41467-022-31432-y>
- 712 Russo, E., & Domeisen, D. I. V. (2023). Increasing Intensity of Extreme Heatwaves: The Crucial Role of Metrics.
713 *Geophysical Research Letters*, *50*(14), e2023GL103540. <https://doi.org/10.1029/2023GL103540>

- 714 Schemm, S., & Röthlisberger, M. (2024). Aquaplanet simulations with winter and summer hemispheres: model
715 setup and circulation response to warming. *Weather and Climate Dynamics*, 5, 43–63.
716 <https://doi.org/10.5194/wcd-5-43-2024>
- 717 Schmidt, D. F., & Grise, K. M. (2021). Drivers of Twenty-First-Century U.S. Winter Precipitation Trends in CMIP6
718 Models: A Storyline-Based Approach. *Journal of Climate*, 34(16), 6875–6889.
719 <https://doi.org/10.1175/JCLI-D-21-0080.1>
- 720 Schumacher, D.L., Singh, J., Hauser, M. *et al.* (2024) Exacerbated summer European warming not captured by
721 climate models neglecting long-term aerosol changes. *Commun Earth Environ* 5, 182.
722 <https://doi.org/10.1038/s43247-024-01332-8>
- 723 Seager, R., Henderson, N., & Cane, M. (2022). Persistent Discrepancies between Observed and Modeled Trends in
724 the Tropical Pacific Ocean. *Journal of Climate*, 35(14), 4571–4584. [https://doi.org/10.1175/JCLI-D-21-](https://doi.org/10.1175/JCLI-D-21-0648.1)
725 [0648.1](https://doi.org/10.1175/JCLI-D-21-0648.1)
- 726 Seager, R., Wu, Y., Cherchi, A., Simpson, I. R., Osborn, T. J., Kushnir, Y., Lukovic, J., Liu, H., & Nakamura, J.
727 (2024). Recent and near-term future changes in impacts-relevant seasonal hydroclimate in the world's
728 Mediterranean climate regions. *International Journal of Climatology*, 1–29.
729 <https://doi.org/10.1002/joc.8551>
- 730 Seth, A., Rauscher, S. A., Biasutti, M., Giannini, A., Camargo, S. J., & Rojas, M. (2013). CMIP5 Projected Changes
731 in the Annual Cycle of Precipitation in Monsoon Regions. *Journal of Climate*, 26(19), 7328–7351.
732 <https://doi.org/10.1175/JCLI-D-12-00726.1>
- 733 Shaw, T. A. (2019). Mechanisms of Future Predicted Changes in the Zonal Mean Mid-Latitude Circulation. *Current*
734 *Climate Change Reports*, 5(4), 345–357. <https://doi.org/10.1007/s40641-019-00145-8>
- 735 Shaw, T. A., P. Arias, M. Collins and Coauthors (2024), Regional Climate Change: consensus, discrepancies, and
736 ways forward, *Frontiers in Climate*, 10.3389/fclim.2024.1391634.
- 737 Shaw, T. A., Baldwin, M., Barnes, E. A., Caballero, R., Garfinkel, C. I., Hwang, Y.-T., Li, C., O’Gorman, P. A.,
738 Riviere, G., Simpson, I. R., & Voigt, A. (2016). Storm track processes and the opposing influences of
739 climate change. *Nature Geoscience*, 9(9), 656–664.
- 740 Shaw, T. A., Barpanda, P., & Donohoe, A. (2018). A moist static energy framework for zonal-mean storm track
741 intensity. *Journal of the Atmospheric Sciences*, 75, 1979–1994. <https://doi.org/10.1175/JAS-D-17-0183.1>

- 742 Shaw, T. A., Miyawaki, O., & Donohoe, A. (2022). Stormier Southern Hemisphere induced by topography and
 743 ocean circulation. *Proceedings of the National Academy of Sciences*, *119*(50), e2123512119.
 744 <https://doi.org/10.1073/pnas.2123512119>
- 745 Shaw, T.A., & Miyawaki, O. (2024). Fast upper-level jet stream winds get faster under climate change. *Nature*
 746 *Climate Change*, *14*, 61–67. <https://doi.org/10.1038/s41558-023-01884-1>
- 747 Shaw, T. A., & Tan, Z. (2018). Testing Latitudinally Dependent Explanations of the Circulation Response to
 748 Increased CO₂ Using Aquaplanet Models. *Geophysical Research Letters*, *45*, 9861–9869.
 749 <https://doi.org/10.1029/2018GL078974>
- 750 Shaw, T. A., Barpanda, P. and A. Donohoe. (2018). A Moist Static Energy Framework for Zonal-Mean
 751 Storm-Track Intensity. *J. Atmos. Sci.*, *75*, 1979–1994. <https://doi.org/10.1175/JAS-D-17-0183.1>
- 752 Shaw, T. A., & Voigt, A. (2016). What can moist thermodynamics tell us about circulation shifts in response to
 753 uniform warming? *Geophysical Research Letters*, *43*(9), 4566–4575.
 754 <https://doi.org/10.1002/2016GL068712>
- 755 Shepherd, T. G. (2014). Atmospheric circulation as a source of uncertainty in climate change projections. *Nature*
 756 *Geoscience*, *7*(10), 703–708. <https://doi.org/10.1038/ngeo2253>
- 757 Shrestha, S., & Soden, B. J. (2023). Anthropogenic weakening of the atmospheric circulation during the satellite era.
 758 *Geophysical Research Letters*, *50*, e2023GL104784. <https://doi.org/10.1029/2023GL104784>
- 759 Simpson, I. R., & Polvani, L.M. (2016). Revisiting the relationship between jet position, forced response, and
 760 annular mode variability in the southern midlatitudes. *Geophysical Research Letters*, *43*, 2896–2903.
 761 <https://doi.org/10.1002/2016GL067989>.
- 762 Simpson, I., Seager, R., Ting, M. & Shaw, T.A. (2016). Causes of change in Northern Hemisphere winter
 763 meridional
 764 winds and regional hydroclimate. *Nature Climate Change*, *6*, 65–70. <https://doi.org/10.1038/nclimate2783>
- 765 Simpson, I. R., McKinnon, K. A., Davenport, F. V., Tingley, M., Lehner, F., Al Fahad, A., & Chen, D. (2021).
 766 Emergent Constraints on the Large-Scale Atmospheric Circulation and Regional Hydroclimate: Do They
 767 Still Work in CMIP6 and How Much Can They Actually Constrain the Future?. *Journal of Climate*, *34*(15),
 768 6355-6377. <https://doi.org/10.1175/JCLI-D-21-0055.1>
- 769 Simpson, I. R., Rosenbloom, N., Danabasoglu, G., Deser, C., Yeager, S. G., McCluskey, C. S., ... & Rodgers, K. B.

- 770 (2023). The CESM2 single-forcing large ensemble and comparison to CESM1: Implications for
771 experimental design. *Journal of Climate*, 36(17), 5687-5711.
- 772 Smith, D. et al. (2022). Attribution of multi-annual to decadal changes in the climate system: The Large Ensemble
773 Single Forcing Model Intercomparison Project (LESFMIP), *Frontiers Climate*, [10.3389/fclim.2022.955414](https://doi.org/10.3389/fclim.2022.955414)
- 774 SPARC, 2022: SPARC Reanalysis Intercomparison Project (S-RIP) Final Report. Masatomo Fujiwara, Gloria L.
775 Manney, Lesley J. Gray, and Jonathon S. Wright (Eds.), SPARC Report No. 10, WCRP-6/2021, doi:
776 [10.17874/800dee57d13](https://doi.org/10.17874/800dee57d13), available at www.sparc-climate.org/publications/sparc-reports.
- 777 Staten, P. W., Grise, K. M., Davis, S. M., Karauskas, K., & Davis, N. (2019). Regional widening of tropical
778 overturning: Forced change, natural variability, and recent trends. *Journal of Geophysical Research:*
779 *Atmospheres*, 124, 6104–6119. <https://doi.org/10.1029/2018JD030100>
- 780 Sun, X., Ding, Q., Wang, S.-Y. S., Topál, D., Li, Q., Castro, C., Teng, H., Luo, R., & Ding, Y. (2022). Enhanced jet
781 stream waviness induced by suppressed tropical Pacific convection during boreal summer. *Nature*
782 *Communications*, 13(1), 1288. <https://doi.org/10.1038/s41467-022-28911-7>
- 783 Tamarin-Brodsky, T., & Kaspi, Y. (2017). Enhanced poleward propagation of storms under climate change. *Nature*
784 *Geoscience*, 10(12), 908–913. <https://doi.org/10.1038/s41561-017-0001-8>
- 785 Tan, Z., & Shaw, T. A. (2020). Quantifying the Impact of Wind and Surface Humidity-Induced Surface Heat
786 Exchange on the Circulation Shift in Response to Increased CO₂. *Geophysical Research Letters*, 47(18),
787 e2020GL088053. <https://doi.org/10.1029/2020GL088053>
- 788 Teng, H., Leung, R., Branstator, G., Lu, J., & Ding, Q. (2022). Warming Pattern over the Northern Hemisphere
789 Midlatitudes in Boreal Summer 1979–2020. *Journal of Climate*, 35(11), 3479–3494.
790 <https://doi.org/10.1175/JCLI-D-21-0437.1>
- 791 Thompson, D. W. J., Solomon, S., Kushner, P. J., England, M. H., Grise, K. M., & Karoly, D. J. (2011). Signatures
792 of the Antarctic ozone hole in Southern Hemisphere surface climate change. *Nature Geoscience*, 4(11),
793 741–749. <https://doi.org/10.1038/ngeo1296>
- 794 Tuel, A., & Eltahir, E. A. B. (2020). Why Is the Mediterranean a Climate Change Hot Spot?. *Journal of Climate*,
795 33(14), 5829-5843. <https://doi.org/10.1175/JCLI-D-19-0910.1>
- 796 Vallis, G. K., P. Zurita-Gotor, C. Cairns, J. Kidston, (2015) Response of the large-scale structure of the atmosphere
797 to global warming, *Q. J. Roy. Met. Soc.*, <https://doi.org/10.1002/qj.2456>.

- 798 Vautard, R., Cattiaux, J., Happé, T., Singh, J., Bonnet, R., Cassou, C., Coumou, D., D’Andrea, F., Faranda, D.,
 799 Fischer, E., Ribes, A., Sippel, S., & Yiou, P. (2023). Heat extremes in Western Europe increasing faster
 800 than simulated due to atmospheric circulation trends. *Nature Communications*, *14*(1), Article 1.
 801 <https://doi.org/10.1038/s41467-023-42143-3>
- 802 Voigt, A., Albern, N., Ceppi, P., Grise, K., Li, Y., & Medeiros, B. (2021). Clouds, radiation, and atmospheric
 803 circulation in the present-day climate and under climate change. *WIREs Climate Change*, *12*, e694.
 804 <https://doi.org/10.1002/wcc.694>
- 805 Voigt, A., & Shaw, T. A. (2015). Circulation response to warming shaped by radiative changes of clouds and water
 806 vapour. *Nature Geoscience*, *8*(2), 102–106. <https://doi.org/10.1038/ngeo2345>
- 807 Watt-Meyer, O., Frierson, D. M. W., & Fu, Q. (2019). Hemispheric Asymmetry of Tropical Expansion Under CO₂
 808 Forcing. *Geophysical Research Letters*, *46*, 9231–9240. <https://doi.org/10.1029/2019GL083695>
- 809 Weisheimer, A., Baker, L. H., Bröcker, J., Garfinkel, C. I., Hardiman, S. C., Hodson, D. L., Palmer, T. N., Robson,
 810 J.
 811 I., Scaife, A. A., Screen, J. A., Shepherd, T. G., Smith, D. M., & Sutton, R. T. (2024). The Signal-to-Noise
 812 Paradox in Climate Forecasts: Revisiting our Understanding and Identifying Future Priorities. *Bulletin of*
 813 *the American Meteorological Society*, <https://doi.org/10.1175/BAMS-D-24-0019.1>
- 814 Williams, R. S., Marshall, G. J., Levine, X., Graff, L. S., Handorf, D., Johnston, N. M., Karpechko, A. Y., Orr, A.,
 815 Van de Berg, W. J., Wijngaard, R. R., & Mooney, P. A. (2024). Future Antarctic Climate: Storylines of
 816 Midlatitude Jet Strengthening and Shift Emergent from CMIP6. *Journal of Climate*, *37*(7), 2157-2178.
 817 <https://doi.org/10.1175/JCLI-D-23-0122.1>
- 818 Wills, R. C. J., Dong, Y., Proistosescu, C., Armour, K. C., & Battisti, D. S. (2022). Systematic Climate Model Biases
 819 in the Large-Scale Patterns of Recent Sea-Surface Temperature and Sea-Level Pressure Change.
 820 *Geophysical Research Letters*, *49*(17), e2022GL100011. <https://doi.org/10.1029/2022GL100011>
- 821 Wills, R.C.J., White, R.H. & Levine, X.J. (2019) Northern Hemisphere Stationary Waves in a Changing Climate.
 822 *Curr Clim Change Rep* **5**, 372–389. <https://doi.org/10.1007/s40641-019-00147-6>
- 823 WMO (World Meteorological Organization), Scientific Assessment of Ozone Depletion: 2018, Global Ozone
 824 Research and Monitoring Project–Report No. 58, 588 pp., Geneva, Switzerland, 2018.
- 825 Woollings, T., Drouard, M., O’Reilly, C.H., Sexton, D.M.H., & McSweeney, C. (2023). Trends in the atmospheric

- 826 jet streams are emerging in observations and could be linked to tropical warming. *Communications Earth*
 827 *& Environment*, 4, 125. <https://doi.org/10.1038/s43247-023-00792-8>
- 828 Wu, Y., Simpson, I. R., & Seager, R. (2019). Intermodel spread in the Northern Hemisphere stratospheric polar
 829 vortex response to climate change in the CMIP5 models. *Geophysical Research Letters*, 46, 13290–13298.
 830 <https://doi.org/10.1029/2019GL085545>
- 831 Yang D., Arblaster J. M., Meehl G. A. and England M. H. (2021). The role of coupled feedbacks in the decadal
 832 variability of the Southern hemisphere Eddy-driven jet, *J. Geophys. Res.* 126 e2021JD035023.
 833 <https://doi.org/10.1029/2021JD035023>
- 834 Yeager, S.G., Chang, P., Danabasoglu, G., Rosenbloom, N., Zhang, Q., Castruccio, F.S., Gopal, A., Rencurrel,
 835 M.C., & Simpson, I.R. (2023). Reduced Southern Ocean warming enhances global skill and signal-to-
 836 noise in an eddy-resolving decadal prediction system. *npj Climate and Atmospheric Science*, 6, 107.
 837 <https://doi.org/10.1038/s41612-023-00434-y>
- 838 Zambri, B., Solomon, S., Thompson, D. W. J., & Fu, Q. (2021). Emergence of Southern Hemisphere stratospheric
 839 circulation changes in response to ozone recovery. *Nature Geoscience*. [https://doi.org/10.1038/s41561-021-](https://doi.org/10.1038/s41561-021-00803-3)
 840 00803-3
- 841 Zaplotnik, Ž., Pikovnik, M., & Boljka, L. (2022). Recent Hadley Circulation Strengthening: A Trend or
 842 Multidecadal Variability?. *Journal of Climate*, 35(13), 4157-4176. [https://doi.org/10.1175/JCLI-D-21-](https://doi.org/10.1175/JCLI-D-21-0204.1)
 843 0204.1
- 844 Zappa, G., & Shepherd, T. G. (2017). Storylines of Atmospheric Circulation Change for European Regional Climate
 845 Impact Assessment. *Journal of Climate*, 30(16), 6561-6577. <https://doi.org/10.1175/JCLI-D-16-0807.1>
- 846 Zappa, G., P. Ceppi, and T. G. Shepherd. (2020) Time-evolving sea-surface warming patterns
 847 modulate the climate change response of subtropical precipitation over land. *Proceedings of the National*
 848 *Academy of Sciences* 117, no. 9: 4539-4545.
- 849 Zhao, X., & Allen, R.J. (2019). Strengthening of the Walker Circulation in recent decades and the role of natural
 850 sea surface temperature variability. *Environmental Research Communications*, 1, 021003.
 851 <https://doi.org/10.1088/2515-7620/ab0dab>.

852

853 **Table 1. Emerging Circulation signals**

854 Atmospheric circulation signals (statistically significant long term trends) that have been
 855 reported in the literature. Following [IPCC terminology](#) signals are labeled detected if the
 856 likelihood of occurrence by chance due to internal variability is small and attributed if the causal
 857 human driver (greenhouse gas, aerosol, ozone forcing, etc.) has been determined.

Signal	Region	Season	Reference	Detected	Attributed
Increased wind shear (zonal wind)	North Atlantic	Annual mean	Lee et al. (2019)		
Upper-troposphere jet strengthening (zonal wind)	Zonal-mean	DJF	Woollings et al. (2023), Franzke & Harnik (2023)		
Lower-troposphere jet strengthening (zonal wind, mean sea level pressure)	North Atlantic	DJF	Blackport & Fyfe (2022), Wills et al. (2022)		
Lower-troposphere jet poleward shift (zonal wind)	Zonal-mean	DJF	Lee & Feldstein (2013), Woollings et al. (2023)	x	x
Mid-troposphere jet weakening (zonal wind)	N. Hemisphere Zonal-mean	JJA	Coumou et al. (2015), Kang et al. (2024b)	x	x
Upper-troposphere jet weakening (zonal wind)	Eurasia	JJA	Dong et al. (2022)	x	x
Storm track weakening (eddy kinetic energy)	N. Hemisphere Zonal-mean	JJA	Coumou et al. (2015), Chang et al. (2016), Gertler & O’Gorman (2019), Kang et al. (2023), Cox et al. (2024), Chemke & Coumou (2024)	x	x
Extratropical cyclone activity weakening (mean sea level pressure)	North Atlantic, North Pacific	JJA	Kang et al. (2024b)	x	x
Increased blocking (500 hPa geopotential height)	Greenland	JJA	Hanna et al. (2018)		
Storm track strengthening (eddy kinetic energy)	S. Hemisphere Zonal-mean	JJA	Chemke et al. (2022)	x	
Storm track strengthening (eddy kinetic energy)	S. Hemisphere Zonal-mean	Annual mean	Shaw et al. (2022), Cox et al. (2024)		

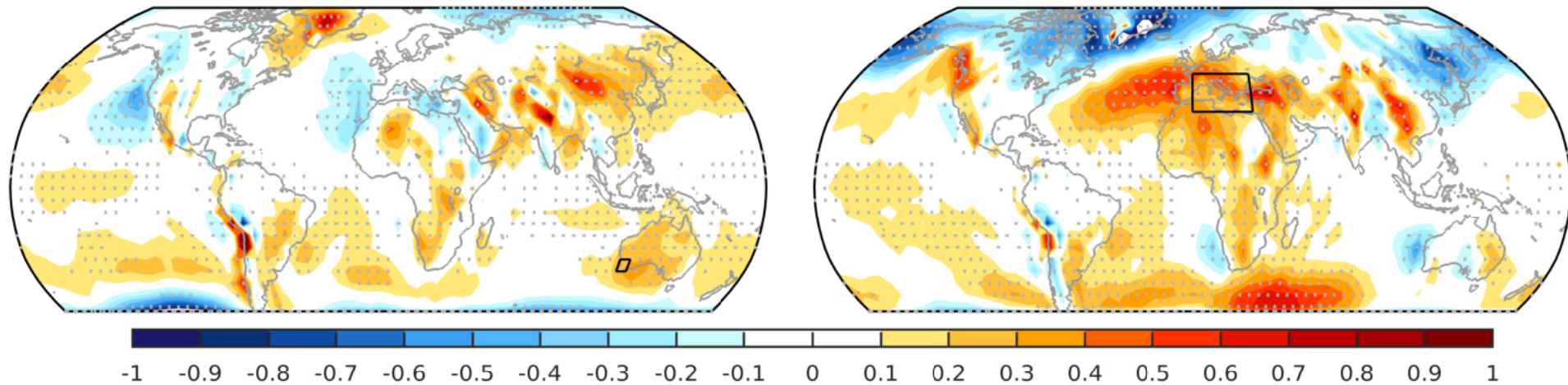
Hadley cell shift (mass stream function)	S. Hemisphere Zonal-mean	Annual mean	Grise et al. (2019), Lionello et al. (2024)	x	x
Hadley cell intensity (mass stream function)	N. Hemisphere Zonal-mean	Annual mean	Chemke & Yuval (2023), Lionello et al. (2024)	x	x
Walker circulation strengthening (mean sea level pressure, surface winds)	Pacific	Annual mean	Chung et al. (2019), Zhao and Allen (2019)	x	
Weakening of upward vertical motion (500 hPa vertical motion)	Global	Annual mean	Shrestha & Soden (2023)	x	x
Increasing sea level pressure	South west Western Australia	JJA	Hope et al (2006); Knutson & Ploshay (2021); Figure 1c	x	
Increasing stationary wave amplitude (200 hPa geopotential height)	N. Hemisphere (200 hPa geopotential height)	JJA	Teng et al. (2022), Sun et al. (2022)		
Strengthening stationary waves (sea level pressure)	Mediterranean	DJF	Tuel & Eltahir (2020); Figure 1d	x	
Strengthening summer Monsoon	N. Hemisphere	JJA	Eyring et al. (2021)		
	Australian	DJF	Borowiak et al (2023); Heidemann et al (2023)	x	

SLP trend (hPa/decade)

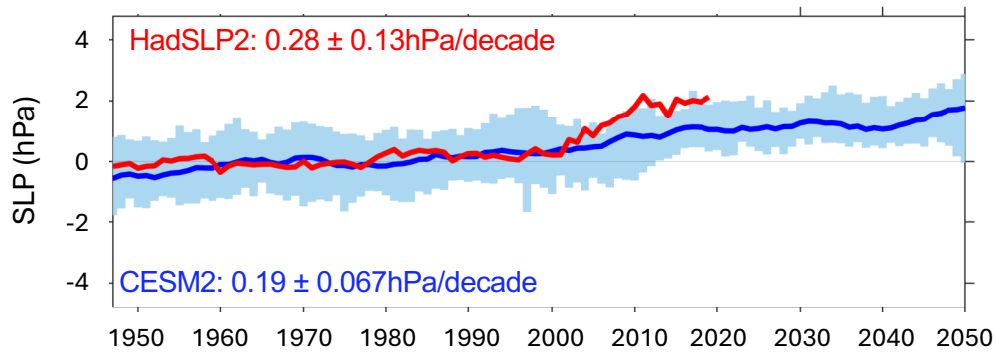
HadSLP2 1950 - 2019

(a) JJA

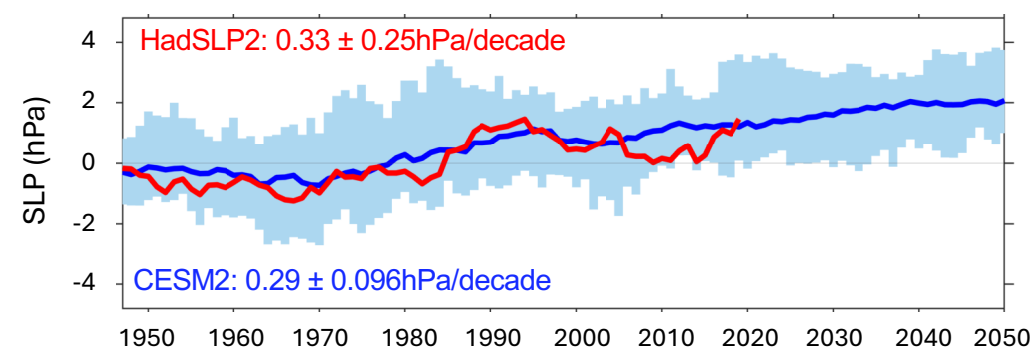
(b) DJF



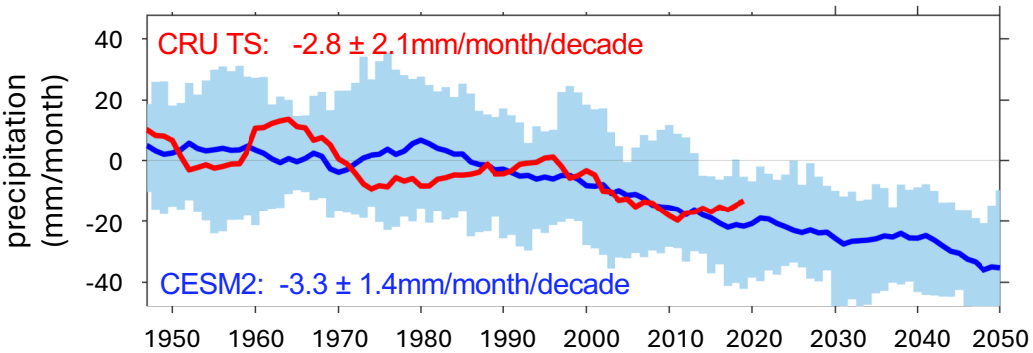
(c) SW Australia [35-30S, 115-120E], JJA



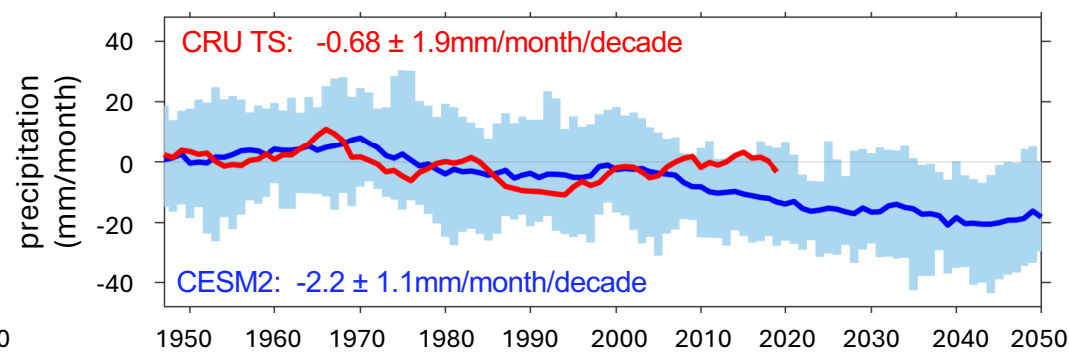
(d) Mediterranean [32-48N, 0-30E], DJF



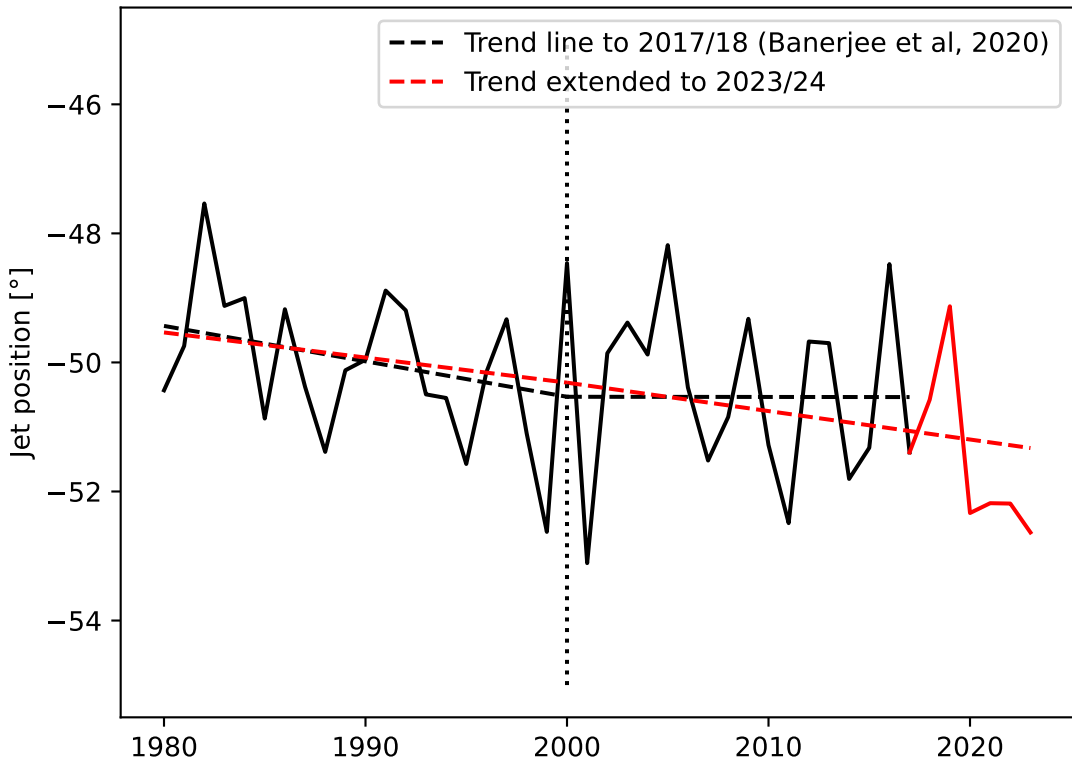
(e) SW Australia [35-30S, 115-120E], JJA



(f) Mediterranean [30-45N, 20-40E], DJF

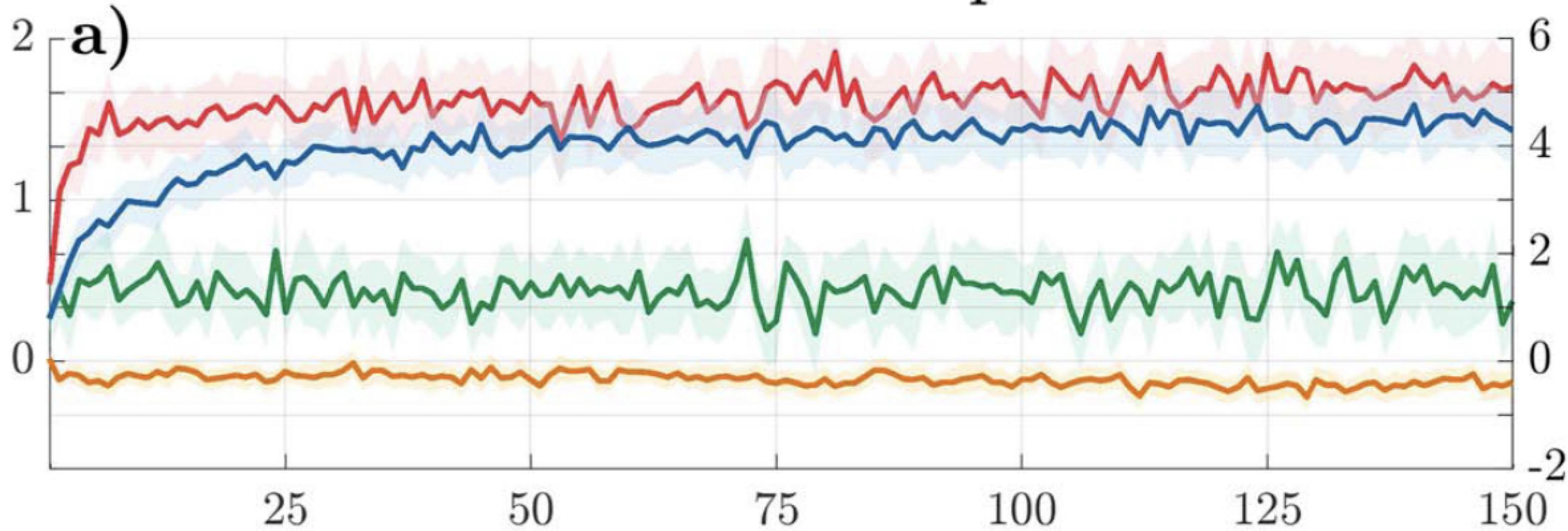


ERA5 1980-2023



Southern Hemisphere

Poleward Shift [$^{\circ}$]



Jet speed trend ($\text{m s}^{-1} \text{ decade}^{-1}$)0.4
0.2
0.0
-0.2
-0.4

44, 303

7, 24

7, 16

9, 29

9, 27

CMIP6

hist-1950-LR

hist-1950-HR

highresSST-present-LR

highresSST-present-HR

